The relationship between past radiative forcings and ENSO activity

Jenna Wollney

Advisor: Dr. Michael Evans

GEOL394

25 November 2019

Abstract

El Niño Southern Oscillation (ENSO) is one of the most influential impacts on the climate of the tropical Pacific, where it occurs, as well as having far-reaching global consequences (Glantz et al., 1991). While ENSO varies irregularly even in the absence of significant external radiative forcings, it is as of yet unclear whether future anthropogenic radiative forcings are likely to have a significant impact on these cycles (Collins et al., 2010). Various studies based on the Zebiak-Cane climate model indicate the likelihood that negative radiative forcings, such as those caused by large volcanic events, will increase the tendency for warm-phase events to occur, as well as the possibility that positive forcings will increase the tendency for cold-phase events (Clement et al., 1996; Adams et al., 2003; D'Arrigo et al., 2006; Mann et al., 2005; Emile-Geay et al., 2008); specifically, Mann et al. (2005) found a tendency for El Niño events to occur in the year following a major eruption (Mann et al., 2005). Precipitation variation in Indonesia is controlled primarily by ENSO, and Indonesian teak tree rings are controlled principally by precipitation; therefore, to test for ENSO variability in any given year, tree ring widths (TRWs) of Indonesian teak (Tectona grandis) trees can be used as a proxy for variation in ENSO (Bijaksana et al., 2007). δ^{18} O analysis of tree rings provides another ENSO variation proxy to analyze for comparison, as δ^{18} O data from tropical tree rings often provides an even more sensitive record to precipitation variations (Schollaen et al., 2015). TRW and δ^{18} O data extend further back in time than rainfall and SST records, and as such, can help extend the historical ENSO record further back in time.

This study used a single factor fixed effects ANOVA to analyze TRWs and δ^{18} O data from Muna teak cores, with the intent of determining whether volcanic forcings increase the likelihood of a warm-phase ENSO event occurring. The analysis determined whether TRWs are significantly narrower or δ^{18} O ratios are significantly higher, indicating occurrence of an El Niño event, for years in which a major volcanic forcing event occurred compared to non-forcing years. Analysis of stable oxygen isotopes was performed on two cores, MUN1.3 and TG01C. Isotopic analysis covered two time periods: 1956-1995, which is a period of overlap for both cores, and 1775-1825, a period that contains stronger eruptions but is only covered by TG01C. In addition to the main analysis, a single factor fixed effects ANOVA and paired t-tests were performed on rainfall data from Harris et al. (2014), with treatments based on ENSO phases as defined by sea surface temperature data from Kaplan et al. (1998). The results of the analysis of annual rainfall data based on ENSO phase indicated that the El Niño phase does result in significant variation in rainfall. Additionally, a correlation analysis was used to determine whether rainfall levels significantly influence TRWs and δ^{18} O values. Tree ring widths were not found to significantly correlate with rainfall data; however, isotope data from TG01C was found to have a significant negative correlation with rainfall, and the lack of significant correlation for MUN1.3 δ^{18} O is suspected to be a result of human error. Despite the presence of significant correlation between TG01C δ^{18} O and rainfall data, the result of the ANOVA based on volcanic forcing data indicates that major volcanic forcing events do not increase the probability of a warm-phase ENSO event occurring. Future work should involve isotopic analysis of more teak increment cores with coverage of more years to get better replication of results.

Table of Contents

Introduction/Background	4
Method of Analysis	5
Presentation of Data and Analysis of Uncertainty	9
Discussion of Results	20
Suggestions for Future Work	21
Conclusions and Broader Implications	22
Acknowledgements	22
References	24
Appendices I-IV	26

List of Figures and Tables

Figure 1: Graph of estimated external radiative forcings from 1400 to 200	(p. 7)
Figure 2: Range of years covered by each increment core and samples per year	(p. 9)
Figure 3: Residual and arstan TRW chronologies	(p. 11)
Figure 4: Volcanic climate forcings from 1750 to 2005	(p. 12)
Figure 5: Volcanic stratospheric sulfur injection from 1567 to 1890	(p. 13)
Figure 6: Average δ^{18} O values for each year for Muna1.3 and TG01C	(p. 14)
Figure 7: Isotope data for MUNA1.3	(p. 15)
Figure 8: Isotope data for TG01C	(p. 16)
Figure 9: TG01C δ^{18} O (per mil VSMOW) vs. rainfall; histogram of residuals	(p. 18)

Introduction and Background Information

ENSO is a climate pattern over the tropical Pacific Ocean that varies irregularly between its neutral phase, its warm phase (El Niño) and its cool phase (La Niña) (Collins et al., 2010). Each phase is caused by variations in sea surface temperature (SST); under normal, neutral phase conditions, the eastern equatorial Pacific Ocean SSTs are cooler than the western SSTs due to upwelling of cool water from the deep ocean, resulting in an east-to-west wind at the ocean surface, as well as rainy conditions at the western side and dry conditions to the east (Collins et al., 2010). The La Niña phase is similar to the neutral phase in that eastern tropical Pacific SSTs are cooler than western SSTs, but to a more intense degree, with a greater contrast in temperature between the two (Collins et al., 2010). However, during the El Niño phase, eastern equatorial Pacific SSTs are anomalously warm, resulting in a weakening or reversal of the east-to-west wind over the Pacific, reduced rainfall in the western equatorial Pacific and increased rainfall to the east (Collins et al., 2010). In fact, one of the most reliable effects of El Niño is a reduction in the amount of rainfall on the western edge of the equatorial Pacific Ocean, particularly in Indonesia (D'Arrigo et al., 2006; Schollaen et al., 2015).

Although it is centered on one part of the globe, ENSO's effects impact climate patterns across Earth in a series of far-reaching effects known as teleconnections, which alter the path of the Jetstream and the intensity of hurricanes in the Pacific and Atlantic Oceans (Glantz et al., 1991). While ENSO varies from year to year under normal conditions (no radiative forcings), it is currently uncertain whether the patterns of its occurrence are significantly affected by radiative forcing that arises from human activities (Collins et al., 2010). It is important to understand how ENSO varies both randomly and in response to forcing events because of both its strong local impact and its effect on severe weather events across the globe (Collins et al., 2010). Knowing how previous forcing events may have impacted ENSO is vital to predicting how future forcing events, such as global warming, might affect both the local intensity of ENSO and its impact on climate patterns across the globe, and thus is necessary for future management of ENSO's effects.

Various studies indicate that volcanic forcing events are correlated with the occurrence of El Niño events (Clement et al., 1996; Adams et al., 2003; D'Arrigo et al., 2006; Mann et al., 2005; Emile-Geay et al., 2008). Mann et al. (2005) use the Zebiak-Cane model (Zebiak and Cane 1987) to determine whether ENSO variability would be significantly impacted by solar and volcanic radiative forcings. Based on the Zebiak-Cane model, negative radiative forcings tend to be correlated to ENSO warm events while positive radiative forcings tend to be correlated to ENSO cool events (Clement et al., 1996; Adams et al., 2003; Mann et al., 2005). The reason for this effect is that uniform radiative cooling tends to decrease the zonal sea surface temperature (SST) gradient, making it more likely to initiate the positive feedbacks between winds, SST, SLP and thermocline depth that lead to warm phase events (Emile-Geay et al., 2008; Clement et al., 1996; Adams et al., 2003; Mann et al., 2005). Mann et al. (2005) found, based on this model, that there was a tendency for El Niño conditions to occur beginning in the year that a major volcanic forcing event occurred, as volcanic events produce negative forcings; isotope data from corals in Palmyra, which are influenced by variations in ENSO, back up this conclusion (Mann et al., 2005). This relationship does seem to be restricted based on the size of eruption events; Emile-Geay et al. (2008) suggest that, based on their analysis using the Zebiak-Cane model, this effect is only likely to occur in the case of eruptions that result in radiative forcings stronger than 3.7 W/m² (Emile-Geay et al., 2008). This study specifically focuses on volcanic forcing events, as

reconstructions by Schurer et al. (2014) indicate that the most significant radiative forcings over the past thousand years were the result of volcanic eruptions and variations in greenhouse gas concentrations (Schurer et al., 2014; see Figure 1).

The historical occurrence of El Niño events can be determined by examining past precipitation levels in Indonesia, as there is a strong correlation between El Niño events and Indonesian droughts (D'Arrigo et al., 2006). Both width and oxygen isotope concentrations of Indonesian teak (*Tectona grandis*) tree rings are controlled strongly by rainfall amount, allowing them to record variations in precipitation; though δ^{18} O values are somewhat more sensitive to variations in precipitation as they are primarily influenced by the inverse relationship between precipitation δ^{18} O values and rainfall amount, while tree ring growth is influenced by other factors as well (Schollaen et al., 2015; Evans, 2007). There are many potential environmental constraints on incremental growth of trees, such as precipitation, temperature, soil moisture, insolation, CO_2 and other nutrients (Cook & Kairiukstis, 1990); however, in Muna, Indonesia, where the set of samples to be used (D'Arrigo, 2010) originate, temperature varies little from year to year, so rainfall is the main controlling factor for tree ring width, as it is for tree ring δ^{18} O, as shown by Bijaksana et al. (2007). Thus, both tree ring width and δ^{18} O record variations in rainfall, and both can be used as proxies for precipitation variations.

Experiment Design and Methods

Tree Ring Width Analysis

My working hypothesis was that the tree ring widths of Indonesian teak increment cores would be significantly narrower during the years in which major volcanic forcings occurred, indicating an increase in warm phase ENSO events, than for years in which there were no major radiative forcings. Thus, my null hypothesis was that the tree ring widths of Indonesian teak increment cores would not be significantly narrower during the years in which major volcanic forcings occurred, indicating that there was no increase in warm phase ENSO events, than for years in which there were no major radiative forcings.

For the portion of the analysis focused on tree ring widths, existing data collected by D'Arrigo et al. (2010) was used. A single factor fixed effects ANOVA was performed using the averaged tree ring width values from D'Arrigo et al. (2010), specifically the residual chronology (Figure 3). The averaged tree ring width values were calculated using tree ring widths measured from increment cores taken from teak trees in Muna, Indonesia at a latitude and longitude -4.8686, 122.7094; elevation is unknown (D'Arrigo et al., 2010). The first treatment consisted of TRWs for years in which major volcanic forcings did occur; replicates of average values were years in the study period in which the 95th percentile of volcanic forcings occurred. The other treatment consisted of TRWs for years in which no major volcanic forcing occurred, and replicates were a random selection of years outside the 95th percentile of volcanic forcings, the number of randomly selected years being equal to the number of years in the first treatment. The test was one-tailed with a critical p value of 0.05. The analysis was run multiple times to ensure that the second treatment more closely represented the array of non-forcing years, as the second treatment runs the risk of randomly representing a skewed portion TRW values. Two analyses were perfored, the first one using volcanic forcing data spanning from 1750 to 2011 from the IPCC AR5 report (IPCC 2013; see Table 1); the second analysis used volcanic stratospheric sulfur injection values from Toohey and Sigl (2017a), a record which extended from 491 BCE to 1890 CE, with the assumption that positive sulfur injection values correspond to negative volcanic forcing values. As the averaged TRW data (D'Arrigo et al., 2010) only covers the

period from 1565 to 2005 CE, only years included in that period were included from either volcanic record. For the IPCC (2013) data, the selected range was 1750 to 2005; for the Toohey and Sigl (2017a) data, the range was 1567 to 1890, as this dataset is not annually resolved and 1567 was the earliest year past 1565 for which a value was recorded. To test for the possibility of a delayed reaction, the same analysis was performed using data from the IPCC AR5 Report, but with a year added to each of the treatment years.

Stable Isotope Analysis

In addition to the tree ring width analysis, a $\delta^{18}O$ analysis was performed, as previous studies have indicated that $\delta^{18}O$ can provide a more precise record of variation in Indonesian precipitation (Schollaen et al., 2015; Evans and D'Arrigo, 2019). ¹⁸O is enriched in tree ring cellulose during droughts, as ¹⁶O is lighter and evaporates preferentially; therefore, Indonesian tree ring $\delta^{18}O$ is expected to be higher during El Niño events, when droughts occur in the region (Evans, 2007; Bijaksana et al., 2007). Thus, the working hypothesis that the $\delta^{18}O$ of Indonesian tree rings would be significantly higher during the years in which major volcanic forcings occurred, indicating a tendency for warm phase ENSO events to occur after major negative forcings, than for years in which there were no major radiative forcings. The corresponding null hypothesis is that the $\delta^{18}O$ of Indonesian tree rings would not be significantly higher during the years in which major volcanic forcings occurred, indicating that there was no increase in warm phase ENSO events, than for years in which there were no major radiative forcings.

The isotope analysis was performed on two teak increment cores, Muna 1.3 and TG01C, which were two of the samples used to develop the tree ring width chronologies used in this study (D'Arrigo et al., 2010); samples were borrowed from collaborator Rosanne D'Arrigo (LDEO, Columbia University). These cores are from teak (*Tectona grandis*) trees in Muna, which is located in the southeastern part of Sulawesi, Indonesia, as these are some of the oldest forests that have demonstrated that they can be successfully dated, and they are likely representative of regional variation in precipitation for tropical Indonesia (Bijaksana et al., 2007). Additionally, precipitation variations in most parts of Indonesia, including Sulawesi Island, are a direct result of ENSO variations, due to Indonesia's location at the western edge of the tropical Pacific Ocean (Bijaksana et al., 2007). The time periods covered by Muna 1.3 and TG01C are 1936-2005 and 1711-1994, respectively. Due to time constraints, only a portion of these years could be analyzed. Two time periods were selected, 1775-1825 from one core and 1957-1994 from both cores, each containing a few major volcanic eruptions (Figure 1). 1957-1994 is a period of overlap between the two cores, allowing data from the two to be compared. Additionally, 1957-1994 is recent enough that there are rainfall and sea surface temperature (SST) records available for the time period, so isotopic results can be analyzed against these more direct measures of variations in ENSO. The second period, 1775-1825, is only covered by one core, TG01C, and there is no overlap with rainfall or SST data; however, the volcanic forcings that occurred during this period are much greater than those that occurred from 1957 to 1994, and there was less positive climate forcing from greenhouse gases then, so there was a possibility that the signal from these events would be stronger. Additionally, though the lack of rainfall and SST data for this time period makes it more difficult to test assumptions, it also means that isotope data collected from this period could help extend the record of ENSO activity further back in time.

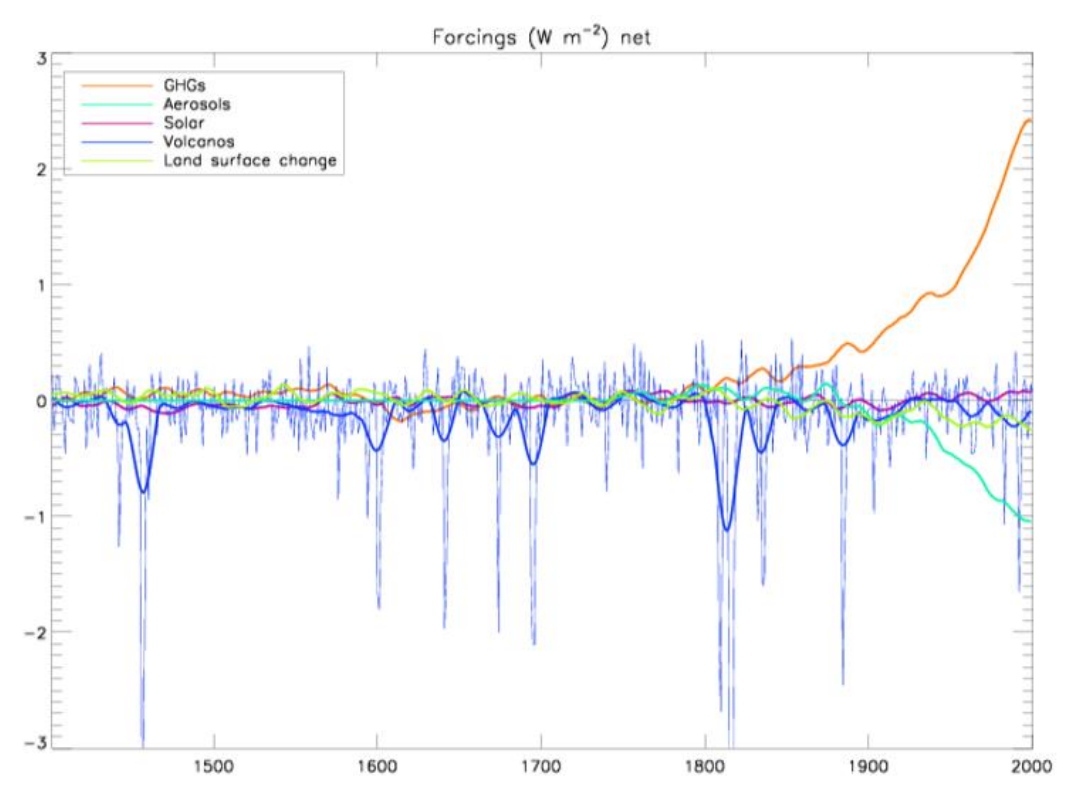


Figure 1: Graph of estimated external radiative forcings from 1400 to 2000, from unpublished work of A.P. Schurer (pers. Comm., 19 October 2018) arising from Schurer et al. (2014). The horizontal scale shows time (years) while the vertical scale shows forcings in W/m². Figure from Evans and D'Arrigo (2019).

The procedure for preparing samples involves microtoming each tree ring, extracting the alpha cellulose from each sample, weighing samples and wrapping them in silver capsules, and analyzing them using the elemental analyzer and gas source isotope ratio mass spectrometer (IRMS) in the Paleoclimate Colaboratory. Before taking any actions that would be destructive towards the cores, the cores were scanned so that they could be checked even after a portion of the wood had already been microtomed. The cores were then visually inspected to check which ring matched up with which year, with tree ring width measurements for each core and markings on the wooden base and on the core as a guide. Notes were made regarding which rings were difficult to distinguish, or especially wide or narrow, for each decade; each core was marked with a penciled dot every decade, and the exact years marked were noted as well. These notes, as well as the tree ring width measurements for each core, were later used as a guide while microtoming the cores. The cores were soaked in hot water to separate them from the bases they were glued to, then dried. The rings analyzed were microtomed by hand rather than with a microtoming machine, as the machine microtomes cores in a straight line, and many of the rings were thin or had a curved shape that would require greater precision. Samples were placed into labelled centrifuge tubes, with any oversized chips being further chopped up first.

The samples then underwent alpha cellulose extraction, as the alpha cellulose is the part of the wood with isotopic values affected by precipitation, and the presence of other wood components in samples could obscure the climate signal (Evans, 2007; Protocol for α -cellulose extraction). The process involves treating samples of microtomed wood with a 1:10 ratio of nitric

acid to acetic acid, heating them, treating them with supernatants, and centrifuging them, before drying them first in an oven around 45-50°C and later in a vacuum desiccator (Protocol for α -cellulose extraction). A papery or cottony white consistency indicated that the extraction had been successful, and that only alpha cellulose remained (Protocol for α -cellulose extraction); brown or tan spots indicate the presence of unprocessed wood. Some lignin often remained unprocessed after extraction, likely due to wood shavings clinging to the centrifuge tube walls away from the acid, so samples were often run through the alpha cellulose extraction process a second time to be sure all non-cellulose components were removed.

Once the samples had sat in the desiccator overnight, they were removed, capped to help keep each sample dry until it could be wrapped and weighed in silver capsules. Samples were weighed at $200 \pm 20~\mu g$, weights were recorded on a chart, and then the capsule containing each sample was closed and rolled into a ball, which was then placed into a sample tray. Slots containing samples in the tray corresponded to the information about each respective sample on the chart. In many cases subsamples for each year were slightly over- or under-weight, so in some cases multiple subsamples for a year were placed into a single capsule, or multiple capsules contained material from a single subsample; this information was recorded on the sample sheets. Care was taken that subsamples from different years did not mix. SAC and AKC Standards were also weighed to $200 \pm 20~\mu g$ and wrapped in silver capsules, then placed into two trays (one for each type of standard) with weights being recorded on charts corresponding to each tray. 15 SAC standards, 12 AKC standards, and about 72 samples were needed for each analysis.

For the analysis of δ^{18} O, both samples and standards were run so data could be normalized, allowing drift in the instrument to be accounted for and comparisons to be made with other datasets (Protocol for analyzing). Samples and standards were loaded into the autosampler in order, which was then purged with helium to remove any remaining traces of air. Sample names and weights along with weights of standards were filled into the run sheet, with care taken to ensure the information in the sheet matched the order of the samples and standards in the autosampler. Samples were left under helium overnight to make sure they were dry before running the analysis. Once each run was started, C and O from the samples were converted into CO via pyrolysis, and CO₂ and H₂O were removed with an acid/water trap before the samples were transferred to the IRMS (Protocol for analyzing). Currents measured for masses 28 (12C16O), 29 (13C16O), and 30 (12C18O) were used to determine isotope ratios (Protocol for analyzing); sample metadata were entered into IonVantage isotopic data acquisition software. The working standards were used for correction of sample data in MATLAB; corrected data were checked for precision, and plots were used to check the correction algorithm (Evans et al., 2016). Uncertainty in the isotopic data was estimated as the standard deviation of replicate corrected working standard data.

Oxygen isotope data were analyzed using a single factor fixed-effects ANOVA, as the tree ring width data were, with one treatment consisting of years in which the 5% most negative volcanic forcings occurred and the other consisting of years randomly selected from the remaining set of years once the treatment years and the 9 years following each were excluded.

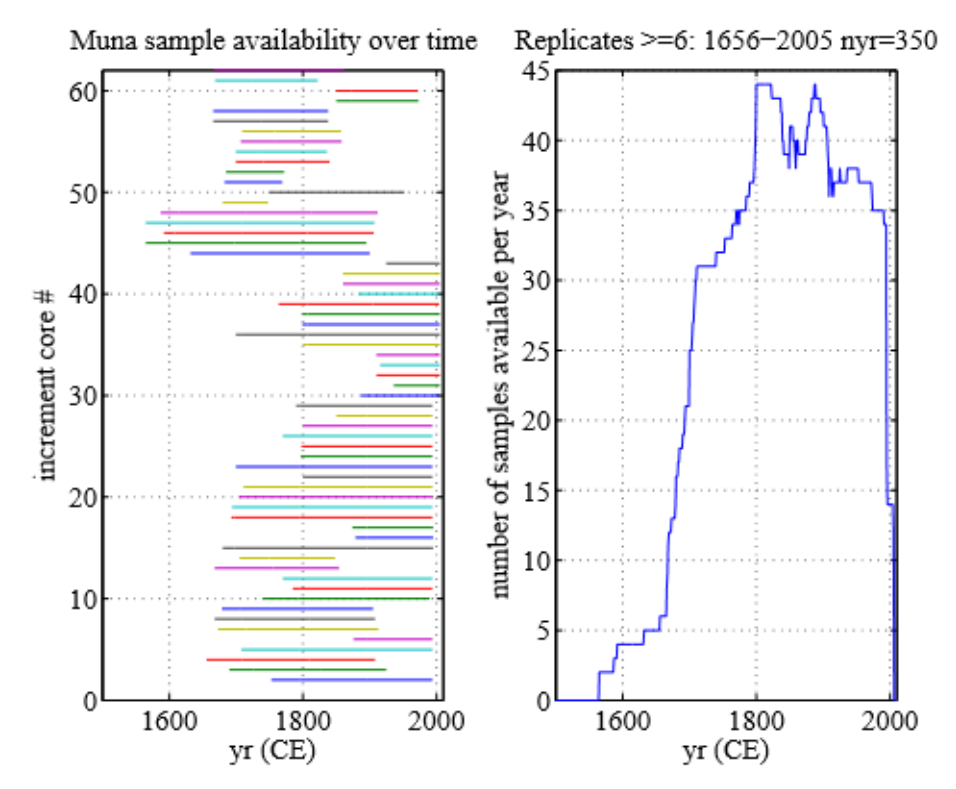


Figure 2: Left: illustration of the range of years covered by each increment core in the dataset from D'Arrigo et al. (2010). Samples were cross-dated to determine ages; the vertical scale is arbitrary. Right: number of samples available for any given year. For the period from 1656 to 2005, at least 6 increment cores are available as replicates for any given year. (From Evans and D'Arrigo (2019))

Presentation of Data and Analysis of Uncertainty

Tree Ring Width Data

To determine which years to use from the IPCC (2013) dataset, the 1750-2005 volcanic forcing data (W/m² vs. year) from the report was used to calculate which years between 1750 and 2005 had volcanic forcings that were significantly more negative than average at pcrit=0.05; the volcanic forcing values for 7 years (1783, 1809, 1815, 1816, 1835, 1884, and 1992) fell outside 1.96 standard deviations of the mean, indicating that the forcings for those years were significantly more negative than the rest of the volcanic forcings. These years were the 7 replicates of the first treatment, which was years in which a major volcanic forcing occurred; for the second treatment, years in which no major forcing occurred, I randomly selected 7 more replicate years from the group that remained after removing the years of the first treatment and the 9 years following each of them, using the MATLAB randperm function. The rationale for removing 10 years including and following each major eruption rather than just the eruption year is that Mann et al. (2005) suggest that volcanic forcings may impact climate variation in the 10 years following an eruption, so in order to avoid violating the assumption of independence of values, it would be necessary to exclude the subsequent decade as well.

For the second analysis using sulfur injection data from Toohey and Sigl (2017a), the same method was used to select the 95th percentile of volcanic sulfur injections between 1567 and 1890; the 5 selected years (1600, 1640, 1783, 1809, and 1815) made up the first treatment. 3 of these years (1783, 1809, and 1815) were also in the 95th percentile of the IPCC (2013) data.

The other three years in the IPCC (2013) 95th percentile that fell inside the total range of Toohey and Sigl (2017a) years (1816, 1835, and 1884) were not large enough to be included in the 95th percentile of the Toohey and Sigl (2017a) data, indicating that the volcanic forcings of 1600 and 1640 were significantly stronger than them. The graphs of both sets of forcing data seem to support this conclusion (Figure 4, 5). To select years for the second treatment, the years from the first treatment and the 9 years following each of them were excluded, as was done for the IPCC (2013) data; 5 years were then randomly selected from those that remained to match the number of replicates in the first treatment.

To restate, my null hypothesis is that ring width variation for years in which major volcanic forcings occurred would be equal to ring width variation for years in which no major forcing occurred, and my working hypothesis is that ring width variation will not be equal between the two sets of years, indicating lower levels of precipitation and the occurrence of a warm-phase ENSO event. I used a single factor fixed effects ANOVA to test this, with a pcrit value of 0.05; to determine the Fcrit value, the degrees of freedom of the Group Mean Square and of the Error Mean Square were used to select the value from a chart of Fcrit values. For the analysis using IPCC (2013) forcing data, the Group Mean Square was 1 and of the Error Mean Square was 12, so the resulting Fcrit was 4.75. For the analysis using Toohey and Sigl (2017a) sulfur injection data, the Group Mean Square was 1 and of the Error Mean Square was 8, so the resulting Fcrit was 5.32.

Due to the fact that the second treatment consists of a selection of randomly selected values, each script was run 20 times to ensure that if the values selected for the second treatment randomly fell within the 5% least likely permutations for a run, it would not skew results. For the analysis using IPCC (2013) forcing data, only one of the 20 F values generated fell outside the range of Fcrit values -4.75<Fcrit<4.75, indicating that 95% of the time there is no significant variation between years in which volcanic forcings occurred and years in which no forcings occurred. The analysis using Toohey and Sigl (2017a) sulfur injection data had the same result, with only one of the 20 F values generated fell outside the range of Fcrit values -5.32<Fcrit<5.32, indicating that 95% of the time there is no significant variation between years in which volcanic forcings occurred and years in which no forcings occurred. These results seem to suggest that the null hypothesis should be accepted.

There were a few assumptions made in performing this ANOVA: it was assumed that only 1 factor explains variation across groups; that variances across groups were homogenous (about equal); that the data was normally distributed; and that there was independence of data within and across groups. The first assumption should be valid for both analyses performed, considering the literature (e.g. Bijaksana et al., 2007) indicate that precipitation is the main controlling factor on Indonesian teak tree ring width, so that should be the only factor explaining variation across groups. The second assumption is may be valid for the analysis using IPCC (2013) data, as the treatment percent variances were generally fairly low, with the highest being 22.6068% over half (13 of the 20 runs) under 5%. It is likely not valid of the analysis using the data from Toohey and Sigl (2017a), however, as the treatment variances for this analysis were higher; for as 11 of the 20 runs the treatment variance went above 10%, with the highest being 36.9386%. The assumption that the data was normally distributed may not be valid. The treatment groups should be independent as the two groups are mutually exclusive, and the removal of the 9 years following the eruption year in addition to the eruption year itself should prevent these likely non-independent years (Mann et al., 2005) from being chosen for the second treatment.

Another assumption made is that the volcanic stratospheric sulfur injection data from Toohey and Sigl (2017a) corresponds to negative volcanic forcing data. This assumption appears to be valid, as the top three years in the 95th percentile were the same for both the Toohey and Sigl (2017a) data and the IPCC (2013) forcing data (Figure 4, 5).

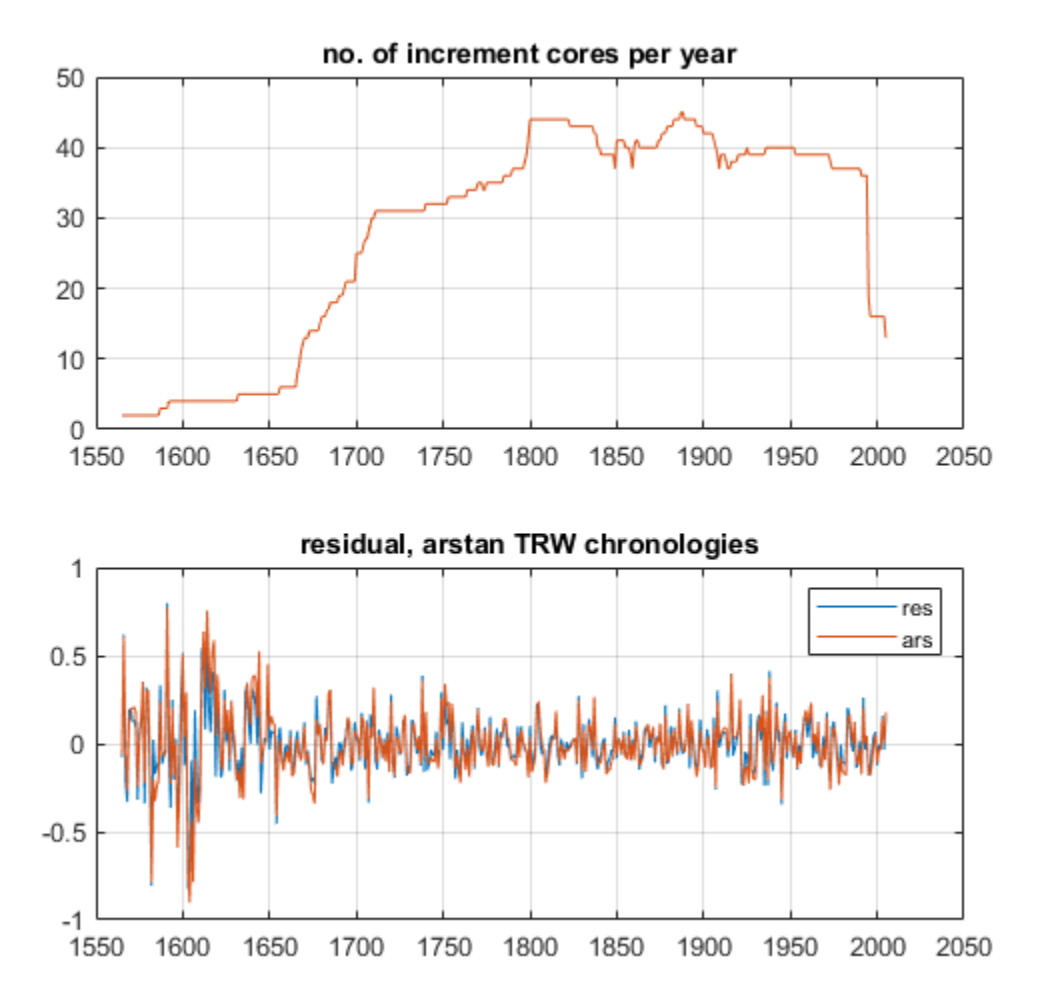
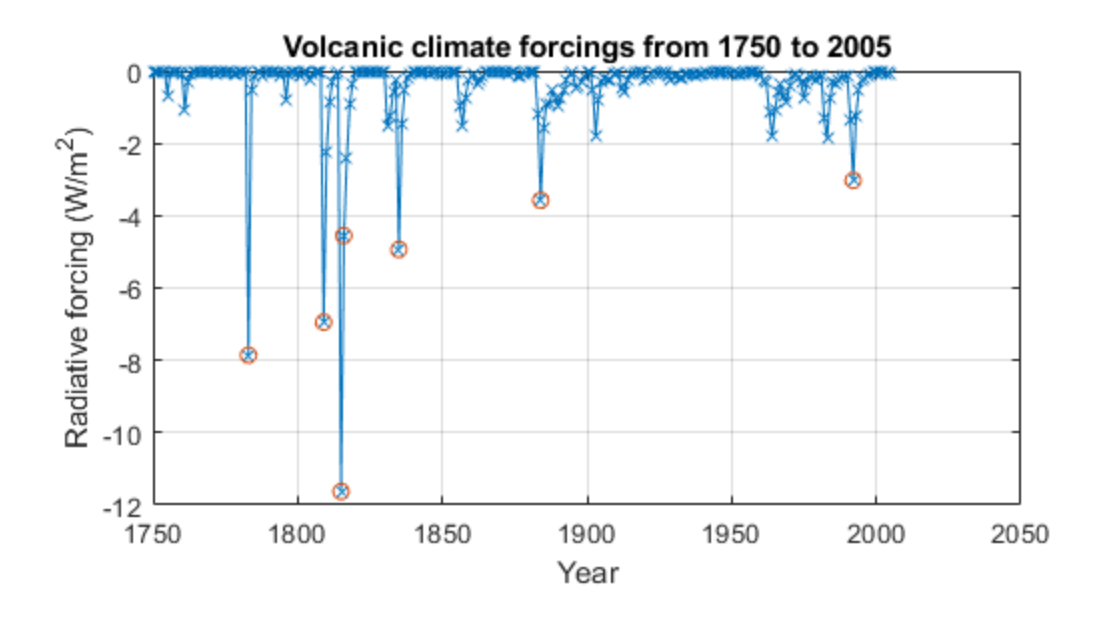


Figure 3: Top: another depiction of number of increment cores available in any given year, lined up with Bottom: residual and arstan TRW chronologies. Increase in variance towards the earlier part of the chronology may be due to a lower sample size of tree cores being used to create that part of the chronology.



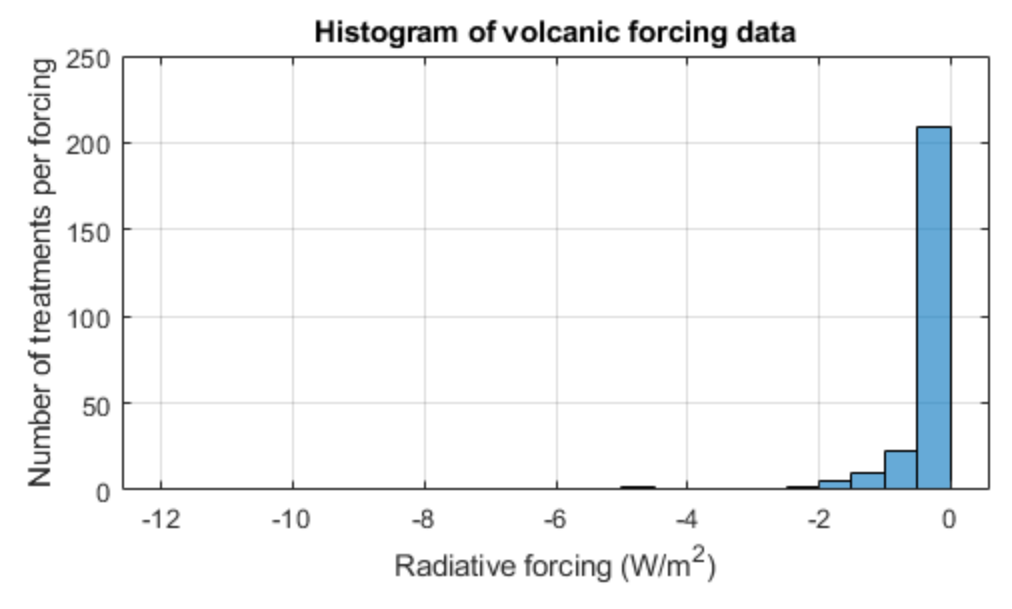
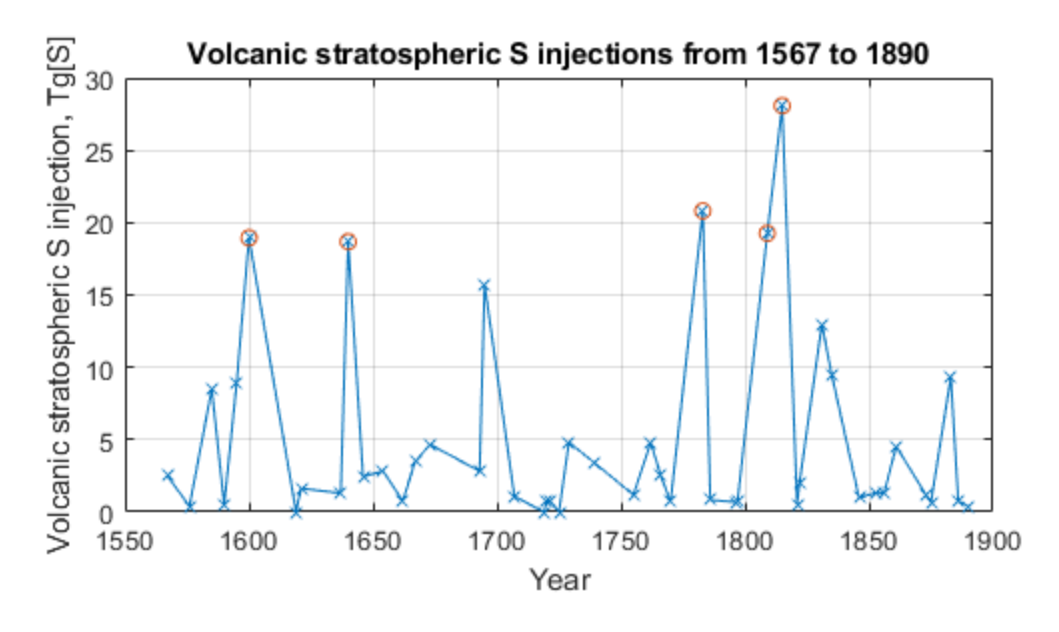


Figure 4: Top: Based on data from the IPCC AR5 report, volcanic climate forcings from 1750 to 2005. The 7 forcings found to be in the 95th percentile are circled in red. Bottom: Histogram of volcanic forcing data; the forcings of most years fall between 0 and -0.5 W/m², with a decrease in years as forcings increase. Graphs created in MATLAB.



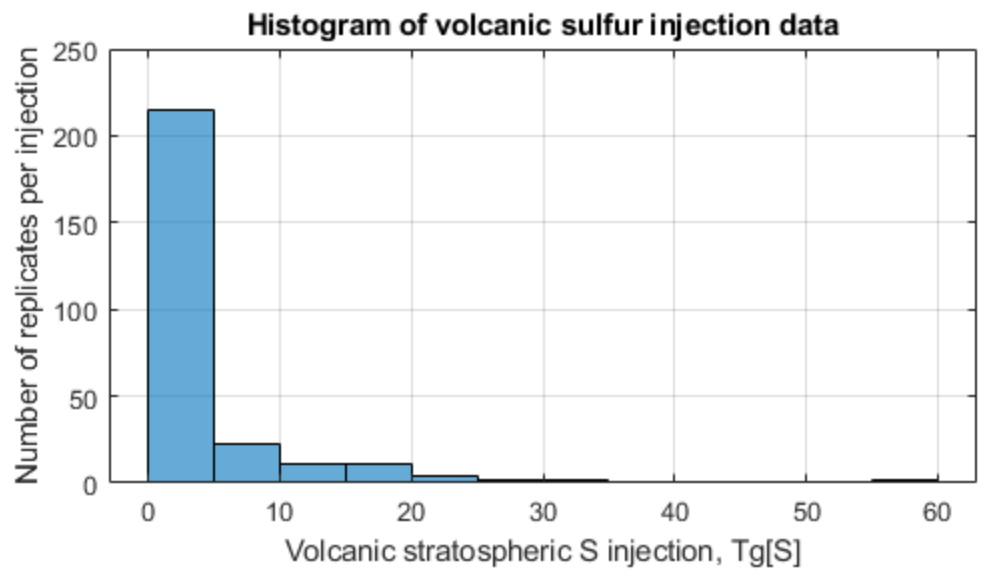


Figure 5: Top: Graph of volcanic stratospheric sulfur injection from 1567 to 1890, based on data from Toohey and Sigl (2017a). Note that, unlike the IPCC AR5 report data, these values are not annually resolved. Positive volcanic stratospheric sulfur injections are assumed to correspond to negative volcanic radiative forcings. The 5 sulfur injections found to be in the 95th percentile are circled in red. Bottom: histogram of volcanic sulfur injection data from 1567 to 1890. The sulfur injection of most years falls between 0 and 5 Tg[S]; the number of years decreases as sulfur injection increases. Graphs created in MATLAB.

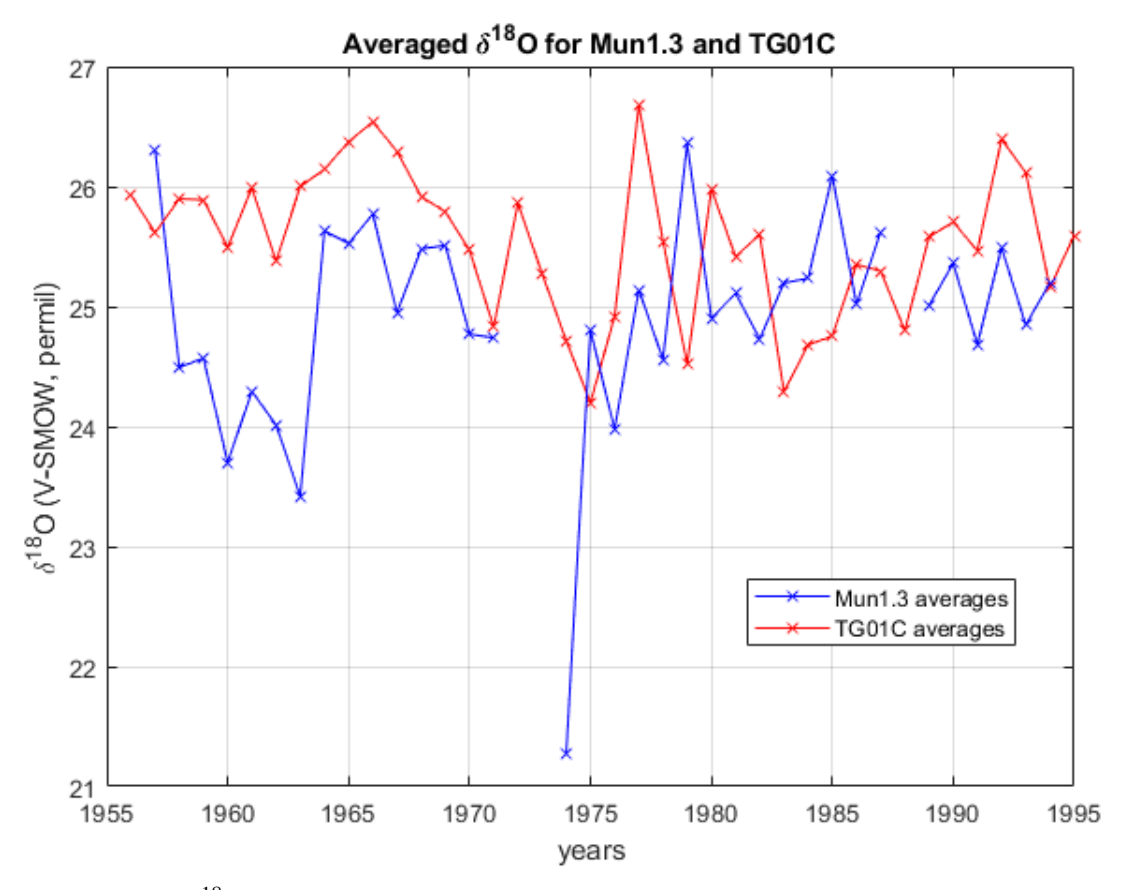


Figure 6: Average $\delta^{18}O$ values for each year for Muna1.3 and TG01C.

$\delta^{18}O$ Data

A range of δ^{18} O values was found for each year for both Muna1.3 (Appendix II) and TG01C (Appendix III and IV), indicating variation in precipitation throughout the year; yearly averaged values were used to perform the analysis, as the exact time of year represented by each subsample was unclear. The δ^{18} O for mun1.3 1974A was not included in the average for that year, as it was anomalously low at 11.95 per mil and fell outside the standard range of δ^{18} O values for plant tissues related to and including cellulose, 19 per mil to 37 per mil (Coplen et al., 2002). As with the TRW data, a single factor fixed effects ANOVA was performed on the isotope data averages. The data collected from Muna 1.3 covered 1957 to 1994, with a few missing years in 1972, 1973, and 1988 (Figure 6, Figure 7); the data collected for TG01C spanned from 1775 to 1825 and from 1956 to 1995 (Figure 6, Figure 8). For 1956 to 1995, there were three years were in the 95th percentile of volcanic forcings: 1964, 1983 and 1992. Isotope values for these years comprised the first treatment for mun1.3; to get the years for the second treatment, 3 years were randomly selected once treatment 1 years and the 9 years that followed each were excluded, as with the analysis of TRWs. Two analyses were performed, one on the full set of isotope data for mun1.3 and one on the full set of TG01C data; each analysis was run 20 times on each dataset to reduce the possibility of random error. For the first analysis, the group mean degrees of freedom was 1 and the error mean degrees of freedom was 4, resulting in a critical F value of 7.71. For Mun1.3, the F ratio fell below the critical F value 60% of the time, indicating that there was no significant difference between δ^{18} O for years in which volcanic

forcings occurred versus those in which no major forcing events occurred. For the ANOVA performed on the combined entire TG01C isotope dataset (1775-1825, 1956-1994), the group mean had 1 degree of freedom while the error mean had 6 degrees of freedom, resulting in a critical F value of 5.99; for all 20 runs of the analysis, the F ratio fell between the critical F value and zero, indicating that there was no significant variation between the two treatments.

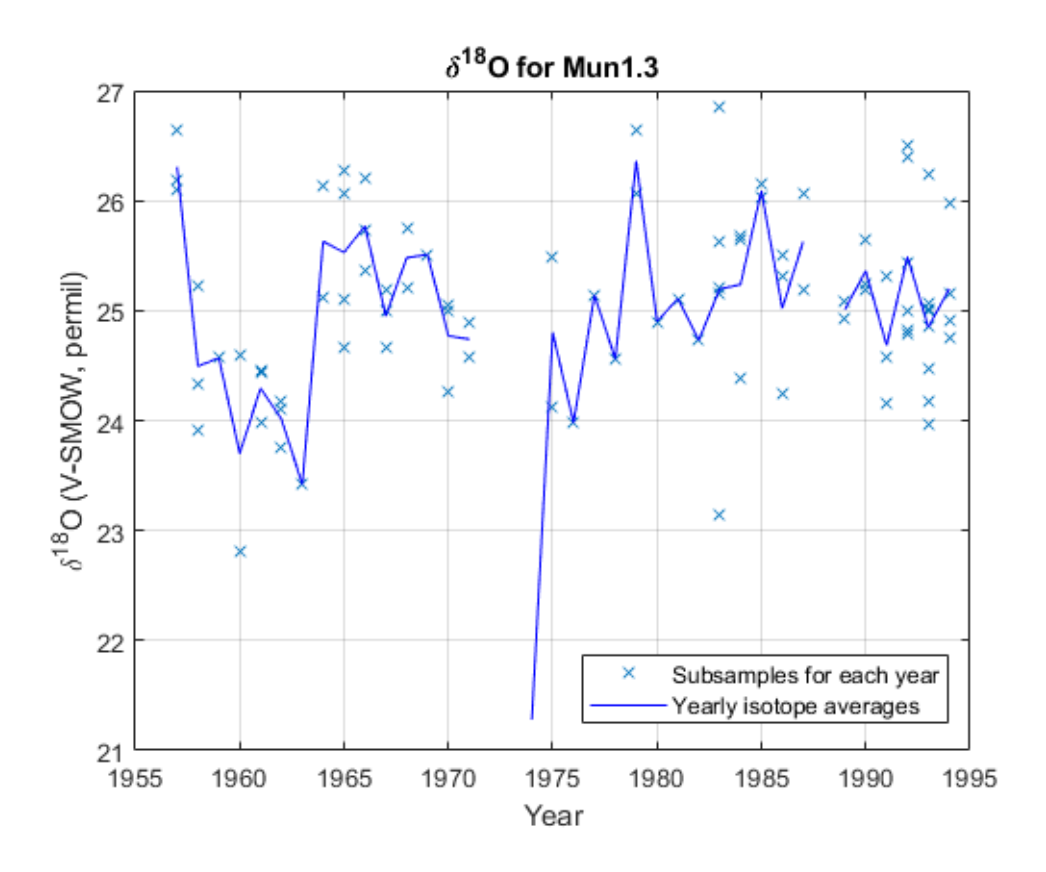
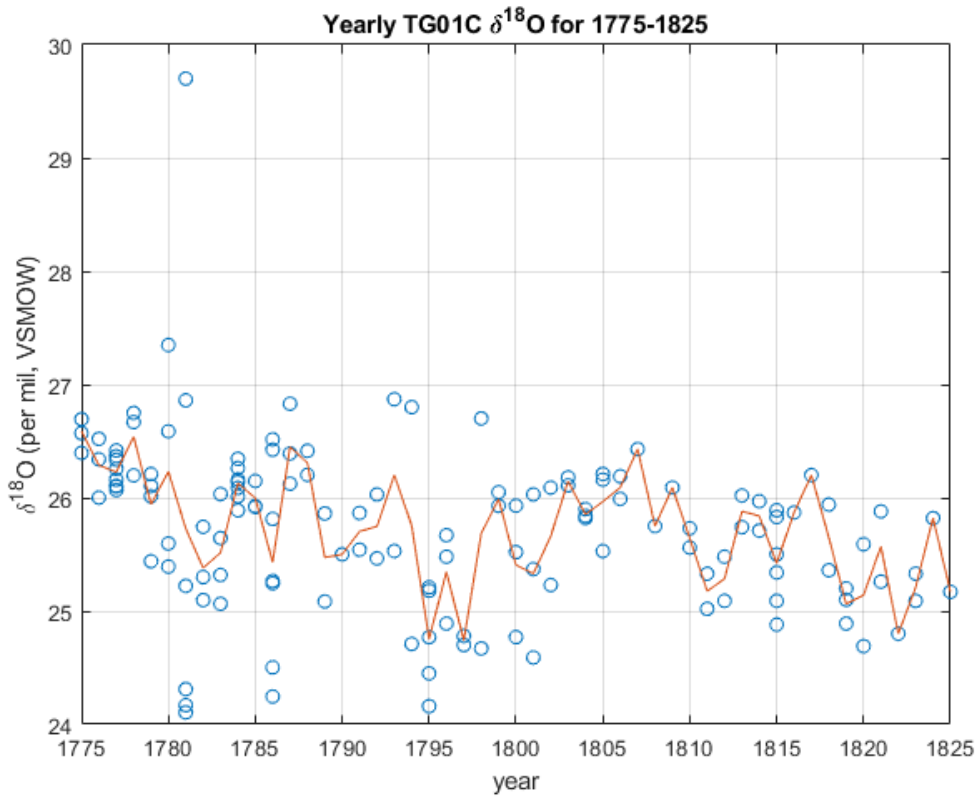


Figure 7: Isotope data for MUNA1.3. The line connects average values of consecutive years; gaps are due to missing samples for 1972-3 and 1989. The value for subsample 1774a is not shown or used for analysis due to its being anomalously low, based on the normal plant tissue δ^{18} O range given by Coplen, et al. (2002).



A. Yearly TG01C δ^{18} O for 1956-1995 28.5 0 28 27.5 27 δ^{18} O (per mil, VSMOW) 0 26.5 26 25.5 25 24.5 φ 24 0 23.5 1955 1985 1960 1965 1970 1975 1990 1980 1995

B. Figure 8: Isotope data for TG01C for a) 1775-1825 and b) 1956-1995. Circles mark the isotope values for subsamples within a given year; the line connects average values of consecutive years.

year

To analyze the uncertainty resulting from the use of proxies, a few different analyses were performed. The relationship between rainfall and ENSO phases was analyzed using a single factor fixed effects ANOVA and paired t tests. Correlation analyses were performed between the δ^{18} O values for both cores studied; between the δ^{18} O values and the core-specific TRWs for each core; and between the δ^{18} O values of each core and the averaged TRW chronology from D'Arrigo et al. (2010). Each test was one-tailed, as correlation was expected to be in a specific direction for each analysis; the pcrit value used was 0.05 for each.

Analysis of Sea Surface Temperature and Rainfall

To test the assumption ENSO causes variation in rainfall levels, a single factor fixed effects ANOVA was performed on the yearly averages from the BMKG rainfall dataset based on SST data from Kaplan et al., 1998. Mean temperature over 3 months is used to determine the phase of ENSO occurring, with warm phase (El Niño) events occurring when the mean anomaly is greater than 0.5°C, cold phase (La Niña) events occurring when the mean anomaly is less than -0.5°C, and the neutral phase occurring when mean SST anomalies fall between the two temperatures ("Equatorial Pacific Sea Surface Temperatures"). Based on this information, yearly SST anomaly data were sorted into three groups (El Niño, La Niña, and Neutral) based on whether they fell above 0.5°C, below -0.5°C, or between the two values. As ENSO phases are officially determined based on three-month averages rather than yearly averages of SST anomalies, these groupings were somewhat imprecise, but an assumption was made that the yearly averages could be used to approximate which phase predominated in any given year. 28 of the years from 1901 to 2005, the range of years covered by both datasets, fell beneath the category of El Niño, 22 beneath La Niña, and 55 beneath the neutral phase. Rainfall data from these years was sorted into three treatments based on ENSO phase; as the treatments needed to be the same size, all 22 La Niña years was used, and a random selection of 22 years each was taken from the El Niño and Neutral categories. Due to the possibility of random error, the test was run 20 times, with pcrit at 0.05. The group mean degrees of freedom was 2 while the error mean degrees of freedom was 63, resulting in an Fcrit value of almost 3.15. The F ratio ranged from 9.9634 to 14.3787, falling above the critical F value for all 20 runs, indicating that there is a significant difference in rainfall values between warm phase years, cold phase years, and neutral phase years. A paired t-test was then run between each set of two treatments to determine which ENSO phases had the most variation in precipitation. Each test was one-tailed, as there was an expected direction for the variation. With 22 replicates, there were 21 degrees of freedom, so the critical t value was 1.721. The test was run ten times, with the t values between the warm and neutral phases and between the warm and cold phases generally falling below -1.721, indicating significant variation between precipitation during the El Niño phase and precipitation occurring during the other two phases. The t value between the cold and neutral phases fell consistently between 0 and 1.721, indicating no significant variation between the La Niña phase and the neutral phase.

Analysis of Rainfall vs. $\delta^{18}O$ and TRWs

To test whether rainfall values in Indonesia significantly influence $\delta^{18}O$ and TRW variation in teak increment cores, a correlation analysis was performed between yearly rainfall averages from the BMKG Rain gauge Station and both the averaged TRW chronology and $\delta^{18}O$ values for each core. The precipitation data is from the Climatic Research Unit Timeseries (CRU

TS) database, which is a monthly record of precipitation in an area (Harris et al., 2014). The specific rainfall data used is from the BMKG rain gauge station, located near Muna, Indonesia. In order to perform the analysis using yearly precipitation, monthly rainfall was added from April to March to get total rainfall for each year; this period was used because unlike the standard calendar year, it covers the Indonesian growing season, when precipitation occurs.

For the analysis of mun1.3 against the yearly averages calculated from the BMKG rainfall record (Harris et al., 2014), there were 33 degrees of freedom, resulting in a critical t value of 1.692, with an expected negative correlation due to ^{18}O being concentrated in the wood during periods of lower rainfall (Evans, 2007). The t value obtained for the correlation coefficient r was -0.6600, which is greater than -1.692 = -tcrit, which indicates that there was no significant correlation between the $\delta^{18}O$ values for mun1.3 and rainfall variations in the region. For the analysis TG01C $\delta^{18}O$ against the rainfall record, there were 38 degrees of freedom, resulting in a critical t value of 1.686, again with an expected negative correlation. The t value obtained for the correlation coefficient r was -2.8565, which is more negative than -tcrit = -1.686, indicating that there was significant negative correlation between the $\delta^{18}O$ of TG01C and rainfall values.

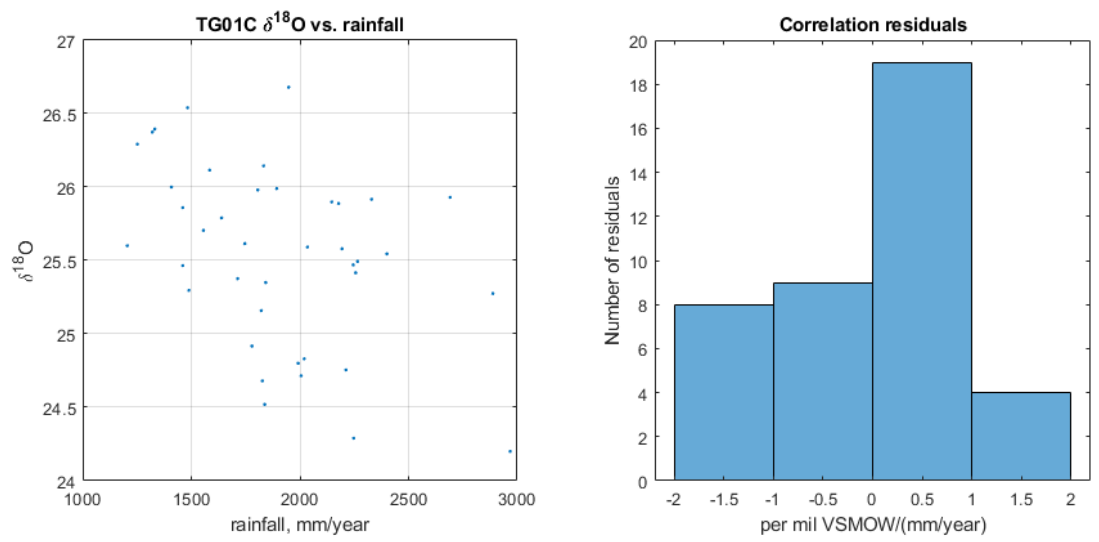


Figure 9: (left) TG01C δ^{18} O (per mil VSMOW) vs. rainfall. A significant negative correlation was found between the two variables. (right) Histogram of correlation residuals; they are not normally distributed.

Correlation analysis between TRWs and $\delta^{18}O$

For the correlation analysis between the averaged TRW chronology (D'Arrigo et al., 2010) and rainfall, there were 103 degrees of freedom, resulting in a critical t value between 1.660 and 1.653, closer to 1.660; the correlation was expected to be positive, as tree rings grow larger during periods of higher precipitation (Cook & Kairiukstis, 1990). The t value obtained for the correlation coefficient r was -0.3429, which is less than 1.660, indicating no significant correlation between the averaged tree ring widths and precipitation.

For the analysis of $\delta^{18}O$ between the two cores, there were 33 degrees of freedom, resulting in a one-tailed critical t value of 1.692 with an expected positive correlation as isotopic concentrations between trees are expected to be influenced by the same factors. The t value

obtained for the correlation coefficient r was 0.7485, between tcrit = 1.692 and 0, indicating that there was no significant correlation between the isotope values obtained for each core.

In the analysis of Mun1.3 δ^{18} O against both the averaged TRW chronology (D'Arrigo et al., 2010) and the TRWs for the individual core, there were 33 degrees of freedom, resulting in a critical t value of 1.692. There was an expected negative correlation, as rainfall variations affect δ¹⁸O and TRW values inversely, with decreases in rainfall leading to increased concentrations of ¹⁸O in tree rings but decreased tree ring growth (Evans, 2007; Cook & Kairiukstis, 1990). The t value obtained for the correlation coefficient r was -0.1270 for the analysis against the averaged chronology and 1.0715 for the analysis against mun1.3 TRWs; in both cases, this result was greater than -tcrit = -1.692, indicating a lack of significant correlation between δ^{18} O for mun1.3 and either tree ring width record. For the analysis of TG01C δ^{18} O against the TRWs for the individual core, there were 88 degrees of freedom, while the analysis of TG01C δ^{18} O against the averaged TRW chronology had 89 degrees of freedom, resulting in a critical t value of 1.662 for both, again with an expected negative correlation. In both cases, the t value obtained for the correlation coefficient r was greater than -tcrit = -1.662, with t = 0.7888 for the analysis against TRWs of the original core and t = -1.5329 for the analysis against the averaged TRW chronology. As with the analysis of mun 1.3 δ^{18} O against TRWs, this indicates that there was no significant correlation between the isotope values and the TRWs.

Analysis of Uncertainty

Tree ring widths and $\delta^{18}O$ of teak cores from Muna, Indonesia are both proxies for rainfall levels in the region, which is itself a proxy for variations in ENSO (Bijaksana et al., 2007; Cook & Kairiukstis, 1990; Evans, 2007). As this analysis uses a proxy of a proxy, it relies on the assumption that each proxy is a good indicator of the signal it is being used to portray. Tree ring widths are affected by other factors such as soil moisture and sunlight, while $\delta^{18}O$ values are influenced by air humidity and soil water in addition to actual precipitation (Cook & Kairiukstis, 1990; Evans, 2007; Schollaen et al., 2015). As such, neither is quite a perfect proxy for rainfall in the region. In addition, there are spatial variations in ENSO, and an El Niño event may occur that affects the eastern Pacific Ocean to a much greater degree than the western Pacific, where the samples used in this study are from (Schollaen et al., 2015). ENSO also varies in intensity; some El Niño events may have a much stronger effect than others, resulting in variations in how much drought occurs in Indonesia during any given event (Schollaen et al., 2015).

There is also uncertainty related to the record of historical volcanic forcings. Radiative forcings caused by volcanic activity are a result of aerosols released into the atmosphere by aerosols, particularly sulphate aerosols due to their long lifetime and effectiveness as scatterers (Myhre et al., 2013). As direct observations of volcanic radiative forcings have only begun fairly recently, historical records of volcanic forcings must be reconstructed from past sulphate aerosol levels; for instance, Toohey and Sigl (2017a, 2017b) use records of sulphate trapped in ice cores from Greenland and Antarctica for their own reconstruction of historical volcanic forcings (Toohey & Sigl, 2017a, 2017b). The sulphate in the ice cores must be used to determine how much sulfur was actually injected into the stratosphere at the time of eruption, thus acting as a proxy; dating of the ice cores used has its own uncertainty as well (Toohey & Sigl 2017b). There is the possibility that there could have been an event that injected sulphate into the atmosphere above the tropical Pacific Ocean that had a strong local effect but was not large enough to result in major sulphate deposits in ice cores. Conversely, a smaller volcanic event that occurred near

the site the ice cores were taken from could potentially result in a deposition of a deceptively large amount of sulphate, which could lead to a larger radiative forcing event being recorded in the historical record even if there was little effect on the tropical Pacific. While Toohey and Sigl (2017a, 2017b) determine approximate latitudes at which eruptions occurred, which should reduce bias related to location and distance from the ice core site, there is still uncertainty due to the fact that this information is determined indirectly, long after the eruptions have occurred. Another possible source of uncertainty in the historical record of volcanic forcings is that sulphate aerosols could have taken longer to settle than expected, which could result in the year for a forcing event to be incorrect.

To test for the possibility that there could be a lag in any effects of volcanic forcings on El Niño, the original TRW analysis was performed but with an extra year added to each of the treatment years in which major forcings occurred. This analysis was run 20 times, with only 4 runs indicating that the null hypothesis should be rejected. As this result only occurs in 20% of the runs, and 80% of the time the null hypothesis was accepted, the results indicate that the null hypothesis should be accepted, even considering the possibility of lag.

Standards were used to correct uncertainty due to drift in the mass spectrometer for each sample run; precisions from these standards were used to calculate uncertainties that remained after data correction. As these precisions represent the variance in the SAC and the AKC standards, they could be used to calculate the standard deviation for the run. The resulting uncertainty was calculated to be 0.47 per mil for the first run; 0.58 for the second run; 0.33 for the third run; 0.22 for the fourth run; and 0.25 for the fifth run. (The run each subsample occurred in is specified in Appendix II, III, and IV.)

Discussion of Results

The results of the single factor fixed-effects ANOVA performed on TG01C isotope data based on radiative forcings seem to indicate that there is no significant difference between the isotope values or TRWs for years in which major volcanic forcings occurred compared to years in which no major volcanic forcings occurred. This, by proxy, indicates that rainfall levels were not significantly lower in Muna, Indonesia during years in which major forcings occurred, which indicates that the forcing event did not result in the occurrence of a warm-phase ENSO event. However, assumptions involved in the analysis must be considered before drawing conclusions.

The lack of significant correlation between the averaged TRW chronology (D'Arrigo et al., 2010) and precipitation indicates that tree ring widths may be sufficiently influenced by other signals that they are not a clear proxy for rainfall in Muna, Indonesia. Therefore, the result of the ANOVA performed on tree ring widths based on radiative forcing data does not appear to reflect on actual variations in precipitation or ENSO.

Isotope data for TG01C did, however, show significant negative correlation with precipitation data, as was expected due to the fact that ¹⁸O is enriched in tree ring cellulose during periods of lower precipitation (Evans, 2007). This result indicates that isotope data is a good proxy for precipitation data and could possibly be used where tree ring widths are complicated by other signals, as has previously been indicated in a study by Schollaen et al. (2015). The fact that the isotope values for mun1.3 do not correlate with rainfall values while those for TG01C do could possibly be attributed to human error; mun1.3 was the first core to be microtomed and extracted, and as such, there was a learning curve involved in sample

preparation. Additionally, several of the mun1.3 samples were extracted only once despite the presence of some unprocessed lignin, and instead an attempt was made to remove remaining lignin chips by hand at the time the samples were wrapped; the possible presence of bits of unprocessed lignin too fine to easily see and remove could have contributed to the resulting isotope values. As it is the δ^{18} O of alpha cellulose that carries the climate signal involving precipitation, the presence of lignin affects isotope values and can obscure the signal (Evans, 2007; Protocol for α -cellulose extraction). Because of the risk of contamination of these samples, the results for mun1.3 are unreliable and will not be the focus of these results.

Rainfall levels in Muna, Indonesia clearly vary with ENSO, with significant variation occurring in precipitation between warm-phase years and cold-phase years as well as between warm-phase years and neutral-phase years, as determined using sea surface temperature data. Considering that there is significant correlation between TG01C isotope data and precipitation data for the region, and that there is significant variation in precipitation related to warm-phase ENSO events, it follows that TG01C isotope data is likely a good proxy for precipitation variations related to warm-phase ENSO events. Thus, the lack of a significant result in the ANOVA performed on TG01C δ^{18} O based on radiative forcing data indicates that there is no significant variation in ENSO related to volcanic forcing events.

However, due to a significant lack of replication in this study, more isotope data should be collected from more tree cores and across more years to further test the analysis. With reliable isotope data from only one teak increment core, there is a greater chance for random error to skew results; as such, analysis of more cores is necessary to be sure whether teak isotope values are a strong proxy for rainfall levels. More cores and more years covered would also allow for a more statistically sound analysis of δ^{18} O variation based on volcanic forcing data by increasing replication both spatially and temporally.

Suggestions for Future Work

There was variation in isotope values within each year, indicating variations in rainfall from month to month. In this study, increment cores were not microtomed exactly enough to know whether each subsample represented a specific slice of time; also, when wrapping samples, multiple samples would be combined if the individual ones did not contain $200 \pm 20 \, \mu g$, which also reduced the clarity of which subsample represented what point within a year. Future analyses could involve carefully microtoming rings into more regular, evenly spaced subsamples to see what sort of variation occurs within a year.

One shortcoming of the analysis of isotope data performed in this project is that the isotope data collected only covered about 91 years (1775-1825 and 1956-1995) due to time constraints; coverage of more years would increase replication of years, resulting in a more reliable analysis. Additionally, this analysis only used two increment cores, and the periods of time covered by the two did not completely overlap; collecting $\delta^{18}O$ data from multiple cores over a single time period would allow for more replication across the sampling site, further reducing uncertainty in the analysis. Future analyses could collect data from more years and across multiple teak cores to increase replication and decrease uncertainty in results.

Another analysis that could be performed in future could focus on whether greenhouse gas forcings have a significant impact on ENSO variability as well. This is slightly more difficult as greenhouse gas forcing has only started to become a major influence on the climate since around the 20th century, and has increased gradually, rather than occurring in short, clear pulses

as volcanic forcings have (Figure 1). Another consideration is that negative radiative forcing due to aerosols has also been increasing in the 20^{th} century and could have some influence on climate effects as well, though it is smaller than positive greenhouse gas forcing during the same time period (Figure 1). Regardless of these complicating factors, it could be interesting to see whether an analysis would reveal any statistically significant variance of $\delta^{18}O$ between years with greenhouse gas forcing and years without. As with the analysis of years with and without volcanic forcings, a single factor fixed effects ANOVA would be used, with one treatment being years in which greenhouse gas forcings occurred and years in which no significant radiative forcings occurred. The replicates for the first treatment would be years with the 95^{th} percentile of greenhouse gas forcings; the replicates for the second treatment would again be a random selection of years in which no significant radiative forcings occurred.

Conclusions and Broader Implications

Based on the ANOVA performed on isotope data based on volcanic forcings, negative radiative forcings caused by major volcanic eruptions do not increase the tendency for warmphase ENSO events to occur. However, this data is based only on data from 91 years, centered on one core; more data is needed to increase spatial and temporal replication of the analysis. El Niño Southern Oscillation has teleconnections that have wide-reaching impacts across the globe (Glantz et al., 1991); the more knowledge there is about this phenomenon, the better we are able to predict how it might change in future. Even knowledge about what factors do not affect ENSO are useful, as knowing what does not cause an effect can be helpful in the path to discovering what does cause it.

Additionally, the results of this analysis seem to indicate variation rainfall in Indonesia is strongly affected by warm-phase ENSO events, as has been shown by Bijaksana et al. (2007). Results of the correlation analyses, however, indicate that tree ring widths are not a good proxy for precipitation in Indonesia or for variations in ENSO, as they lack correlation with rainfall data. However, oxygen isotope values of tree ring cellulose do seem to correlate with regional rainfall, and thus may be useful for extending the record of rainfall and ENSO data further back in time. Isotope data may allow more reliable records to be produced than TRWs, as supported by these results and by Schollaen et al. (2015). This information could help produce more accurate historical records of precipitation and related climate events in future.

Acknowledgements

I would like to acknowledge Adaire Nehring and Urjoshi Nahid, who both worked in the Paleoclimate Laboratory with me to help prepare samples; Adaire also provided technical help and moral support. I would also like to acknowledge my advisor, Dr. Evans, for all his help and support, and for providing me with the basis for my project.

I pledge on my honor that I have not given or received any unauthorized assistance on this assignment.

References

- Adams, J. B., Mann, M. E., & Ammann, C. M. (2003). Proxy evidence for an El Niño-like response to volcanic forcing. *Nature*, 426(6964), 274.
- Bijaksana, S., Ngkoimani, L. O., D'Arrigo, R., Krusic, P., Palmer, J., Sakulich, J., & Zulaikah, S. (2007). Status of tree-ring research from teak (*Tectona grandis*) for climate studies. *J Geofisika*, 2, 1-7.
- Clement, A. C., Seager, R., Cane, M. A., & Zebiak, S. E. (1996). An ocean dynamical thermostat. *Journal of Climate*, *9*(9), 2190-2196.
- Collins, M., An, S. I., Cai, W., Ganachaud, A., Guilyardi, E., Jin, F. F., Jochum, M., Lengaigne, M., Power, S., Timmermann, A., Vecchi, G., & Wittenberg, A. (2010). The impact of global warming on the tropical Pacific Ocean and El Niño. *Nature Geoscience*, *3*(6), 391.
- Coplen, T. B., Hopple, J. A., Böhlke, J. K., Peiser, H. S., Rieder, S. E., Krouse, H. R., Rosman, K. J. R., Ding, T., Vocke, Jr., R. D., Révész, K. M., Lamberty, A., Taylor, P., & De Bièvre, P. U.S. Geological Survey. (2002). *Compilation of Minimum and Maximum Isotope Ratios of Selected Elements in Naturally Occurring Terrestrial Materials and Reagents* (Water-Resources Investigations Report 01-4222).
- Cook, E. R., & Kairiukstis, L. A. (Eds.). (1990). *Methods of Dendrochronology: Applications in the Environmental Sciences*. Springer Science & Business Media.
- D'Arrigo, R., Wilson, R., Palmer, J., Krusic, P., Curtis, A., Sakulich, J., Bijaksana, S., Zulaikah, S., & Ngkoimani, L. O. (2006). Monsoon drought over Java, Indonesia, during the past two centuries. *Geophysical Research Letters*, 33(4).
- D'Arrigo, R. D., Krusic, P.J., & Palmer, J. G. (2010), D'Arrigo Muna, Sulawesi TEGR ITRDB INDO005, *Tech. rep.*, NOAA, National Centers for Environmental Information, https://www.ncdc.noaa.gov/paleo-search/study/12628.
- Emile-Geay, J., Seager, R., Cane, M. A., Cook, E. R., & Haug, G. H. (2008). Volcanoes and ENSO over the past millennium. *Journal of Climate*, 21(13), 3134-3148.
- Equatorial Pacific Sea Surface Temperatures (n.d.). Retrieved from https://www.ncdc.noaa.gov/teleconnections/enso/indicators/sst/
- Evans, M. N. (2007), Toward forward modeling for paleoclimatic proxy signal calibration: a case study with oxygen isotopic composition of tropical woods, *Geochemistry*, *Geophysics*, *Geosystems*, 8(7), doi: 10.1029/2006GC001406.
- Evans, M. N., Selmer, K. J., Breeden III, B. T., Lopatka, A. S., & Plummer, R. E. (2016). Correction algorithm for online continuous flow δ13C and δ18O carbonate and cellulose stable isotope analyses. *Geochemistry, Geophysics, Geosystems*, 17(9), 3580-3588.
- Evans, M. N. (2019), D'Arrigo. R. D. P2C2: Collab. Research: Hydroclimatic response of ENSO to natural and anthropogenic radiative forcing. [Personal communication]
- Glantz, M. H., Katz, R. W., & Nicholls, N. (Eds.). (1991). *Teleconnections linking worldwide climate anomalies* (Vol. 535). Cambridge: Cambridge University Press.
- Harris, I. P. D. J., Jones, P. D., Osborn, T. J., & Lister, D. H. (2014). Updated high-resolution grids of monthly climatic observations—the CRU TS3. 10 Dataset. *International journal of climatology*, *34*(3), 623-642.
- IPCC, 2013: Annex II: Climate System Scenario Tables [Prather, M., G. Flato, P. Friedlingstein, C. Jones, J.-F. Lamarque, H. Liao and P. Rasch (eds.)]. In: Climate Change 2013: The Physical Science Basis. Contribution of Working Group I to the Fifth Assessment Report of the Intergovernmental Panel on Climate Change [Stocker, T.F., D. Qin, G.-K. Plattner, M. Tignor, S.K. Allen, J. Boschung, A. Nauels, Y. Xia, V. Bex and P.M. Midgley (eds.)].

- Cambridge University Press, Cambridge, United Kingdom and New York, NY, USA.
- Kaplan, A., M. Cane, Y. Kushnir, A. Clement, M. Blumenthal, and B. Rajagopalan, Analyses of global sea surface temperature 1856-1991, *Journal of Geophysical Research*, **103**, 18,567-18,589, 1998
- Mann, M. E., Cane, M. A., Zebiak, S. E., & Clement, A. (2005). Volcanic and solar forcing of the tropical Pacific over the past 1000 years. *Journal of Climate*, 18(3), 447-456.
- Myhre, G., D. Shindell, F.-M. Bréon, W. Collins, J. Fuglestvedt, J. Huang, D. Koch, J.-F. Lamarque, D. Lee, B. Mendoza, T. Nakajima, A. Robock, G. Stephens, T. Takemura and H. Zhang, 2013: Anthropogenic and Natural Radiative Forcing. In: *Climate Change 2013: The Physical Science Basis. Contribution of Working Group I to the Fifth Assessment Report of the Intergovernmental Panel on Climate Change* [Stocker, T.F., D. Qin, G.-K. Plattner, M. Tignor, S.K. Allen, J. Boschung, A. Nauels, Y. Xia, V. Bex and P.M. Midgley (eds.)]. Cambridge University Press, Cambridge, United Kingdom and New York, NY, USA.
- Protocol for α-cellulose extraction from wood (KJA-1). Retrieved from http://one.geol.umd.edu/intranet/Protocols/Costech-IRMS/cellulose_extraction.html on 21 February 2019.
- Protocol for analyzing cellulose samples for $\delta^{13}C$ and $\delta^{18}O$ on the Costech-IRMS. Retrieved from http://one.geol.umd.edu/intranet/Protocols/Costech-IRMS/Costech_d13C_d18O_analysis.html on 22 April 2019.
- Protocol for cellulose data processing. Retrieved from http://one.geol.umd.edu/intranet/Protocols/Costech-IRMS/Cellulose_data_correction_modular.html on 23 April 2019.
- Protocol for Microtoming. Retrieved from http://one.geol.umd.edu/intranet/Protocols/Costech-IRMS/microtome.html on 21 February 2019.
- Protocol for using the electronic leak detector. Retrieved from http://one.geol.umd.edu/intranet/Protocols/Costech-IRMS/Scanning_Wood_Cores.html on 21 February 2019.
- Schollaen, K., Karamperidou, C., Krusic, P., Cook, E., & Helle, G. (2015). ENSO flavors in a tree-ring δ^{18} O record of *Tectona grandis* from Indonesia. *Climate of the Past Discussions*, 10(5), 3965-3987.
- Schurer, A. P., Tett, S. F., & Hegerl, G. C. (2014). Small influence of solar variability on climate over the past millennium. *Nature Geoscience*, 7(2), 104. doi: 10.1038/ngeo2040.
- Toohey, Matthew; Sigl, Michael (2017a). Reconstructed volcanic stratospheric sulfur injections and aerosol optical depth, 500 BCE to 1900 CE, version 2. World Data Center for Climate (WDCC) at DKRZ. https://doi.org/10.1594/WDCC/eVolv2k_v2
- Toohey, M. & Sigl, M. (2017b). Volcanic stratospheric sulfur injections and aerosol optical depth from 500 BCE to 1900 CE, Earth Syst. Sci. Data, 9, 809–831, https://doi.org/10.5194/essd-9-809-2017
- Zebiak, S. E., & Cane, M. A. (1987). A Model El Niño-Southern Oscillation. *Monthly Weather Review*, 115(10), 2262-2278.

Appendix I

ear	W/m^2	Year	W/m^2	Year	W/m^2	Year	W/m^2
1750	-0.001	1814	0	1878	-0.075	1942	-0.
1751	0	1815	-11.629	1879	-0.05	1943	-0.
1752	0	1816		1880		1944	-0.0
1753	0	1817	-2.419	1881	-0.025	1945	-0.0
1754	0	1818	-0.915	1882	-0.025	1946	-0.0
1755	-0.664	1819	-0.337	1883	-1.175	1947	-0.0
1756	0	1820	-0.039	1884	-3.575	1948	-0.0
1757	0	1821	0.033	1885	-1.575	1949	-0.07
1758	0	1822	0	1886	-0.9	1950	-0.07
1759	0	1823	0	1887	-0.925	1951	-0.0
1760	-0.06	1824	0	1888	-0.55	1952	-0
1761	-1.093	1825	0	1889	-0.725	1953	-0.07
1762	-0.3	1826	0	1890	-0.975	1954	-0
1763	-0.093	1827	0	1891	-0.975	1955	-0.0
1764		1828	0	1892	-0.75	1956	
	-0.021						-0.02
1765	-0.003	1829	0	1893	-0.225	1957	-0.02
1766	0	1830	0	1894	-0.1	1958	
1767	0	1831	-1.538	1895	-0.025	1959	
1768	0	1832	-1.229	1896	-0.45	1960	-0.1
1769	0	1833	-0.605	1897	-0.425	1961	-0.2
1770	0	1834	-0.223	1898	-0.3	1962	-0.32
1771	0	1835	-4.935	1899	-0.125	1963	-1.:
1772	-0.07	1836	-1.445	1900	-0.05	1964	-1
1773	-0.02	1837	-0.523	1901	-0.025	1965	-1.0
1774	-0.005	1838	-0.192	1902	-0.5	1966	-0.5
1775	-0.001	1839	-0.069	1903	-1.8	1967	-0.3
1776	0	1840	-0.047	1904	-0.8	1968	-0.6
1777	0	1841	-0.013	1905	-0.325	1969	-0.8
1778	-0.067	1842	-0.003	1906	-0.175	1970	-0.4
1779	-0.071	1843	-0.052	1907	-0.225	1971	-0.3
1780	-0.018	1844	-0.014	1908	-0.25	1972	-0
1781	-0.004	1845	-0.003	1909	-0.1	1973	-0
1782	-0.001	1846	-0.071	1910	-0.075	1974	-0.32
1783	-7.857	1847	-0.02	1911	-0.05	1975	-0.
1784	-0.522	1848	-0.005	1912	-0.475	1976	-0.
1785	-0.121	1849	-0.001	1913	-0.6	1977	-0.1
1786	-0.027	1850	-0.1	1914		1978	-C
1787	-0.002	1851	-0.075	1915	-0.1	1979	-0.2
1788	-0.133	1852	-0.025	1916	-0.075	1980	-0.1
1789	-0.041	1853	-0.025	1917	-0.05	1981	-0.1
1790	-0.009	1854	0	1918	-0.05	1982	-1.3
1791	-0.001	1855	-0.05	1919	-0.05	1983	-1.8
1792	0.001	1856	-0.975	1920	-0.225	1984	-0.
1793	0	1857	-1.5	1921	-0.223	1985	-0.3
1794	-0.157	1858		1922	-0.2	1986	-0.3
1795	-0.137	1859		1923		1987	-0. -0.
1796	-0.781	1860		1924		1988	-0
1797	-0.071	1861		1925		1989	-0.
1798	-0.016	1862	-0.35	1926		1990	-0.
1799	-0.002	1863	-0.25	1927	-0.05	1991	-1.
1800	0	1864	-0.125	1928	-0.125	1992	-3.0
1801	-0.154	1865	-0.05	1929	-0.25	1993	-1.2
1802	-0.048	1866		1930		1994	-(
1803	-0.011	1867	0	1931	-0.125	1995	-0.
1804	-0.23	1868	0	1932	-0.2	1996	-0.1
1805	-0.07	1869	-0.025	1933	-0.175	1997	-0.1
1806	-0.016	1870		1934		1998	-0.0
1807	-0.002	1871	-0.025	1935	-0.1	1999	-0.
1808	0	1872	-0.025	1936	-0.075	2000	-0.
1809	-6.947	1873	-0.075	1937	-0.075	2001	-0.
1810	-2.254	1874	-0.05	1938	-0.125	2002	-0.
1811	-0.836	1875	-0.025	1939	-0.1	2003	-0.0
1812	-0.308	1876	-0.15	1940		2004	-0.
1813	-0.109	1877	-0.125	1941	-0.05	2005	-0.0

Table 1: Volcanic radiative forcings from the IPCC AR5 report (IPCC, 2013)

Appendix II: Table of Muna1.3 Isotope Data (1957-1994)

position sample_ID	date_time	RT	amplitude	mass	c13	o18	c13c	o18c	run	Subsamples included	year	Letter in run plan
10 20191007mun_1_3_1957A.raw	10/7/2019 14:43	345	5.54	212	27.62217	27.6841	-25.00	26.10		1 L1A M1A D2A	1957	A
11 20191007mun_1_3_1957B.raw	10/7/2019 14:58	345.3	5.33	193	27.6777	28.28088	-24.96	26.64		1 L1A M1A D2A L2A	1957	В
12 20191007mun_1_3_1957C.raw	10/7/2019 15:12	345.7	5.44	193	27.58653	27.82978	-25.05	26.18		1 L2A T2A	1957	С
13 20191007mun_1_3_1958A.raw	10/7/2019 15:26	345.9	5.46	196	26.34305	25.92146	-26.22	24.34		1 G1A M1A	1958	A
14 20191007mun_1_3_1958B.raw	10/7/2019 15:40	345.3	5.22	193	26.45367	25.50366	-26.13	23.91		1 S1A Y1A	1958	В
15 20191007mun_1_3_1958C.raw	10/7/2019 15:54	345.2	5.22	190	26.69216	26.93075	-25.91	25.23		1 S1A Y1A	1958	С
16 20191007 mun_1_3 1959A.raw	10/7/2019 16:08	345.9	5.30	191	26.60543	26.27115	-26.00	24.57		1 D G J	1959	A
17 20191007 mun_1_3 1960A.raw	10/7/2019 16:23	345.8	5.83	207	26.63722	24.44751	-25.98	22.81		1 E I	1960	A
18 20191007 mun_1_3 1960B.raw	10/7/2019 16:37	344.9	5.46	192	27.49649	26.35959	-25.19	24.59		1 EIM	1960	В
19 20191007 mun 1 3 1961A.raw	10/7/2019 16:51	345.3	5.01	183		26.21487		24.43		1 G	1961	A
20 20191007 mun 1 3 1961B.raw	10/7/2019 17:05	345.5	5.20			26.28079		24.46		1 G I	1961	В
21 20191007 mun 1 3 1961C.raw	10/7/2019 17:19	345.8	5.17	185	26.9301	25.81241	-25.74	23.99		1 G I K	1961	С
22 20191007 mun 1 3 1962A.raw	10/7/2019 17:33	345.8	6.13	219	26.6678	25.97979	-25.99	24.11		1 D	1962	A
23 20191007 mun 1 3 1962B.raw	10/7/2019 17:47	345.7	5.36	185	26.55684	25.63659	-26.11	23.76		1 G	1962	В
24 20191007 mun 1 3 1962C.raw	10/7/2019 18:02	345.4	5.88	202	26.43502	26.0932	-26.23	24.17		1 J O	1962	С
25 20191007 mun 1 3 1963A.raw	10/7/2019 18:16	345.6	5.57	198	26.6896	25.33708	-26.00	23.42		1 DEG	1963	A
11 20191021 mun 1 3 1964A.raw	10/22/2019 14:35					25.96675				2 A E	1964	
10 20191021 mun 1 3 1964B.raw	10/22/2019 14:21	345.1	5.28	0.181	25.67883	24.92888	-25.89	25.12		2 E	1964	В
12 20191021 mun 1 3 1965A1.raw			6.19	0.211	25.92805	26.11894	-25.66	26.27		2 E G	1965	A1
13 20191021mun_1_3_1965B1.raw						24.97931				2 E G L	1965	
26 20191007 mun 1 3 1965A.raw	10/7/2019 18:30									11	1965	
27 20191007 mun 1 3 1965B.raw	10/7/2019 18:44					28.19286				1 L	1965	
28 20191007 mun 1 3 1966A.raw	10/7/2019 18:58					28.36577				1 E	1966	
29 20191007 mun 1 3 1966B.raw	10/7/2019 19:13					27.89503				1 EHL	1966	
30 20191007 mun 1 3 1966C.raw	10/7/2019 19:27					27.52244				1 L O	1966	
31 20191007 mun 1 3 1967A.raw	10/7/2019 19:41					27.16201				1 A	1967	
32 20191007 mun 1 3 1967B.raw	10/7/2019 19:55									1 A D	1967	
33 20191007 mun 1 3 1967C.raw	10/7/2019 20:09					27.41659				1 D	1967	
40 20191007 mun 1 3 1968A.raw	10/7/2019 21:49					27.57938		-		1 A	1968	
41 20191007 mun 1 3 1968B.raw	10/7/2019 22:03					28.16389				1 E	1968	
42 20191007 mun 1 3 1969A.raw	10/7/2019 22:17					27.92703				1 A	1969	
43 20191007 mun 1 3 1970A.raw	10/7/2019 22:32					27.45854				1 A D	1970	
44 20191007 mun 1 3 1970B.raw	10/7/2019 22:46					27.41772				1 A D	1970	
45 20191007 mun 1 3 1970C.raw	10/7/2019 23:00					26.64947				1 A D	1970	
46 20191007 mun 1 3 1971A.raw	10/7/2019 23:14					27.00933				1 A C	1971	
47 20191007 mun 1 3 1971B.raw	10/7/2019 23:29									1 C E	1971	
48 20191007 mun 1 3 1974A.raw	10/7/2019 23:43				19.97429					1 C D	1974	
49 20191007 mun 1 3 1974B.raw	10/7/2019 23:57					23.56473				1 D E F	1974	
50 20191007 mun 1 3 1975A.raw	10/8/2019 0:11					28.00268				1 D H K	1975	
51 20191007 mun 1 3 1975B.raw	10/8/2019 0:26				-	26.57338				1 D H K N	1975	

52 20191007mun_1_3_1976A.raw	10/8/2019 0:40	345.8	5.23	194 26.54986	26.44403	-26.28	23.98	1 F J O	1976 A
53 20191007mun_1_3_1977A.raw	10/8/2019 0:54	345.3	6.29	219 26.747	27.66826	-26.10	25.14	1 C F H	1977 A
54 20191007mun_1_3_1978A.raw	10/8/2019 1:09	344.9	5.48	189 26.54365	27.06984	-26.30	24.56	1 C F	1978 A
55 20191007mun_1_3_1979A.raw	10/8/2019 1:23	345.1	5.01	184 27.15741	29.28065	-25.73	26.65	1 A D	1979 A
56 20191007mun_1_3_1979B.raw	10/8/2019 1:37	345.2	6.08	209 27.06584	28.67937	-25.82	26.07	1 A D E	1979 B
57 20191007mun_1_3_1980A.raw	10/8/2019 1:51	345.7	5.31	191 26.57455	27.45393	-26.28	24.90	1 B C	1980 A
58 20191007mun_1_3_1981A.raw	10/8/2019 2:06	345.9	5.06	180 26.26605	27.67668	-26.57	25.11	1 B C D	1981 A
59 20191007mun_1_3_1982A.raw	10/8/2019 2:20	346	5.39	195 26.28979	27.28357	-26.55	24.73	1 A B C	1982 A
60 20191007mun_1_3_1983A.raw	10/8/2019 2:34	345.6	5.72	205 26.52941	27.73129	-26.33	25.15	1 D	1983 A
61 20191007mun_1_3_1983B.raw	10/8/2019 2:49	345.3	5.73	207 26.85421	28.24257	-26.03	25.63	1 G I	1983 B
62 20191007mun_1_3_1983C.raw	10/8/2019 3:03	344.9	5.77	217 27.55196	29.54193	-25.37	26.86	1 G I M	1983 C
63 20191007mun_1_3_1983D.raw	10/8/2019 3:17	345.4	5.02	187 27.24271	27.801	-25.67	25.20	1 Q	1983 D
70 20191007mun_1_3_1983E.raw	10/8/2019 4:58	345.7	5.92	216 26.73776	25.6477	-26.15	23.14	1 Q T	1983 E
71 20191007mun_1_3_1984A.raw	10/8/2019 5:12	345.7	5.09	194 26.56102	26.96198	-26.31	24.38	1 C E	1984 A
72 20191007mun_1_3_1984B.raw	10/8/2019 5:27	345.2	5.72	200 27.06107	28.33803	-25.85	25.68	1 GILN	1984 B
73 20191007mun_1_3_1984C.raw	10/8/2019 5:41	345	5.61	191 26.99044	28.30168	-25.91	25.65	1 GILN	1984 C
74 20191007mun_1_3_1985A.raw	10/8/2019 5:56	345	5.67	214 27.04247	28.83885	-25.86	26.15	1 A C	1985 A
75 20191007mun_1_3_1985B.raw	10/8/2019 6:10	344.9	5.09	198 27.36596	28.71108	-25.56	26.03	1 E	1985 B
76 20191007mun_1_3_1986A.raw	10/8/2019 6:24	345.4	5.93	218 27.83677	28.15126	-25.12	25.50	1 B	1986 A
77 20191007mun_1_3_1986B.raw	10/8/2019 6:39	345.7	5.58	210 27.49617	27.95953	-25.44	25.32	1 B C	1986 B
78 20191007mun_1_3_1986C.raw	10/8/2019 6:53	346.2	5.14	205 26.69963	26.82462	-26.18	24.24	1 B C F G	1986 C
79 20191007mun_1_3_1987A.raw	10/8/2019 7:08	345.1	5.10	197 26.78356	28.74981	-26.10	26.06	1 A C	1987 A
80 20191007mun_1_3_1987B.raw	10/8/2019 7:22	345	4.91	184 26.61999	27.82593	-26.26	25.19	1 A C E	1987 B
81 20191007mun_1_3_1989A.raw	10/8/2019 7:37	346.2	5.90	207 26.50565	27.72146	-26.36	25.09	1 B C D	1989 A
82 20191007mun_1_3_1989B.raw	10/8/2019 7:51	346.4	5.96	214 26.17147	27.55703	-26.68	24.93	1 B C D E	1989 B
14 20191021mun_1_3_1990A.raw	10/22/2019 15:18	344.7	5.14 0	.184 24.74178	25.14429	-26.84	25.24	2 A B	1990 A
15 20191021mun_1_3_1990B.raw	10/22/2019 15:32	344.8	5.83 0	.199 24.99271	25.57705	-26.60	25.65	2 C D	1990 B
16 20191021mun_1_3_1990C.raw	10/22/2019 15:49	345.2	5.60 0	.195 24.91063	25.14329	-26.69	25.19	2 C D E	1990 C
17 20191021mun_1_3_1991A.raw	10/22/2019 16:27	344.9	5.91 0	.205 24.85093	25.28472	-26.76	25.31	2 B	1991 A
18 20191021mun_1_3_1991B.raw	10/22/2019 17:21	345.4	5.82 0	.197 24.73272	24.57838	-26.88	24.58	2 B D1A	1991 B
19 20191021mun_1_3_1991C.raw	10/22/2019 17:37	345.6	5.51 0	.211 24.36041	24.18319	-27.26	24.16	2 B D1A D1B E1A	1991 C
20 20191021mun_1_3_1992A.raw	10/22/2019 17:55	345.1	6.17 0	.209 23.91767	24.87819	-27.70	24.83	2 B	1992 A
21 20191021mun_1_3_1992B.raw	10/22/2019 18:09	345.4	6.02 0	.201 24.38602	25.4919	-27.25	25.43	2 C	1992 B
22 20191021mun_1_3_1992C.raw	10/22/2019 18:42	344.6	5.72 0	.202 25.52699	26.57461	-26.14	26.50	2 C E	1992 C
23 20191021mun_1_3_1992D.raw	10/22/2019 18:59	344.9	5.77	0.19 25.53857	26.49378	-26.13	26.40	2 C E FGH	1992 D
24 20191021mun_1_3_1992E.raw	10/22/2019 19:13	345.7	6.30 0	.209 24.90061	25.12124	-26.77	25.00	2 1	1992 E
25 20191021mun_1_3_1992F.raw	10/22/2019 19:50	345.3	5.84 0	.197 24.95731	24.9275	-26.72	24.78	2 FGH I	1992 F

26 20191021mun_1_3_1993A.raw	10/22/2019 20:06	345.1	5.25	0.183	24.28541	25.17815	-27.38	25.01	2	В	1993	4
27 20191021mun_1_3_1993B.raw	10/22/2019 20:22	344.3	5.83	0.187	24.78283	26.41462	-26.90	26.24	2	В	1993 E	3
28 20191021mun_1_3_1993C.raw	10/22/2019 21:15	345.3	5.71	0.191	23.97643	24.66846	-27.70	24.47	2	C1A	1993 (3
29 20191021mun_1_3_1993D.raw	10/22/2019 22:01	345.6	5.46	0.205	25.14231	25.20642	-26.56	24.99	2	B C1A D	1993 [)
30 20191021mun_1_3_1993E.raw	10/22/2019 22:16	345.6	6.12	0.209	24.77494	24.41336	-26.93	24.18	2	B C1A D	1993 E	
31 20191021mun_1_3_1993F.raw	10/22/2019 22:30	344.4	6.06	0.211	25.20369	25.3171	-26.51	25.07	2	Е	1993 F	:
32 20191021mun_1_3_1993G.raw	10/22/2019 22:44	345	5.89	0.203	25.32649	25.10833	-26.40	24.85	2	F	1993 (ì
33 20191021mun_1_3_1993H.raw	10/22/2019 22:58	345.6	5.97	0.21	25.04043	24.24607	-26.68	23.97	2	F	1993 H	1
40 20191021mun_1_3_1994A.raw	10/23/2019 0:39	345.2	6.03	0.205	24.91518	26.31136	-26.84	25.98	2	A B1A	1994	4
41 20191021mun_1_3_1994B.raw	10/23/2019 0:53	345.6	5.62	0.19	24.44041	25.49297	-27.30	25.15	2	B1A B1B	1994 E	3
42 20191021mun_1_3_1994C.raw	10/23/2019 1:07	345.2	5.39	0.187	24.42903	25.26391	-27.32	24.91	2	B1A B1B C	1994 (
92 20191021mun_1_3_1994D.raw	10/23/2019 13:37	344.2	5.91	0.205	25.33926	25.53218	-26.68	24.75	2	С	1994 [)

Appendix III: Table of TG01C Isotope Data, 1956-1995:

position	sample_ID	date_time	RT	amplitude	mass	c13	o18	c13c	o18c	run	subsamples included	year	assigned letter
43	20191021tg01c_1956B.raw	10/23/2019 1:21	344.5	5.74	0.21	26.50951	26.28052	-25.28	25.93		2 A C	1956	В
44	20191021tg01c_1957A.raw	10/23/2019 1:46	345.4	5.32	0.187	25.27832	25.42974	-26.49	25.07		2 B	1957	Α
45	20191021tg01c_1957B.raw	10/23/2019 2:00	345.6	5.17	0.185	25.18281	25.31654	-26.59	24.95		2 A	1957	В
46	20191021tg01c_1957C.raw	10/23/2019 2:15	344.6	5.37	0.194	25.54402	25.86736	-26.24	25.50		2 A	1957	С
47	20191021tg01c_1957D.raw	10/23/2019 2:29	344.7	5.25	0.181	25.90882	27.30232	-25.88	26.94		2 B C	1957	D
48	20191021tg01c_1958A.raw	10/23/2019 2:48	345.1	5.60	0.193	25.5743	26.91536	-26.21	26.55		2 A	1958	Α
49	20191021tg01c_1958B.raw	10/23/2019 3:03	345.4	5.83	0.204	25.59642	26.52654	-26.19	26.15		2 A	1958	В
50	20191021tg01c_1958C.raw	10/23/2019 3:27	345.7	5.51	0.191	25.55234	26.31412	-26.24	25.93		2 A B	1958	С
51	20191021tg01c_1958D.raw	10/23/2019 3:42	345.4	5.84	0.214	25.59566	26.4762	-26.20	26.09		2 B C	1958	D
52	20191021tg01c_1958E.raw	10/23/2019 3:56	345.7	5.54	0.198	24.90498	25.16486	-26.88	24.77		2 B C D	1958	E
53	20191021tg01c_1959A.raw	10/23/2019 4:10	345.2	5.55	0.19	25.67733	26.38724	-26.12	26.00		2 A	1959	Α
54	20191021tg01c_1959B.raw	10/23/2019 4:25	345	5.95	0.207	26.00677	27.25078	-25.80	26.87		2 B	1959	В
55	20191021tg01c_1959C.raw	10/23/2019 4:39	345.5	6.09	0.197	25.57908	26.7635	-26.22	26.37		2 A B	1959	С
56	20191021tg01c_1959D.raw	10/23/2019 4:53	345.3	5.78	0.188	25.23458	25.62806	-26.56	25.23		2 C	1959	D
57	20191021tg01c_1959E.raw	10/23/2019 5:08	344.5	5.23	0.183	26.05172	25.67832	-25.76	25.27		2 D	1959	E
58	20191021tg01c_1959F.raw	10/23/2019 5:22	345.3	6.16	0.213	26.1215	25.99765	-25.70	25.59		2 C D	1959	F
59	20191021tg01c_1960A.raw	10/23/2019 5:36	345.8	6.31	0.215	25.81073	24.68133	-26.01	24.26		2 A	1960	Α
60	20191021tg01c_1960B.raw	10/23/2019 5:51	344.5	5.83	0.194	26.60083	26.86114	-25.23	26.45		2 C D1A	1960	В
61	20191021tg01c_1960C.raw	10/23/2019 6:05	345.5	5.59	0.196	26.64067	26.18117	-25.20	25.77		2 D1A	1960	С
62	20191021tg01c_1961A.raw	10/23/2019 6:24	344.9	5.33	0.19	26.69165	26.23669	-25.15	25.82		2 A	1961	Α
63	20191021tg01c_1961B.raw	10/23/2019 6:38	345.1	5.80	0.194	26.65158	26.68473	-25.19	26.26		2 B1A	1961	В
70	20191021tg01c_1961C.raw	10/23/2019 8:19	345.1	5.20	0.19	26.74931	26.64633	-25.13	26.17		2 B1A B1B	1961	С
71	20191021tg01c_1961D.raw	10/23/2019 8:33	344.8	5.63	0.204	26.83877	26.26741	-25.05	25.78		2 B1A B1B C1A	1961	D
72	20191021tg01c_1961E.raw	10/23/2019 8:48	344.6	5.37	0.193	26.59973	26.3796	-25.29	25.88		2 B1A B1B C1A C1B	1961	E
73	20191021tg01c_1961F.raw	10/23/2019 9:02	344.4	5.90	0.206	27.07063	26.53384	-24.83	26.03		2 D	1961	F
74	20191021tg01c_1962A.raw	10/23/2019 9:17	344.4	5.58	0.2	27.05879	26.14399	-24.85	25.62		2 A	1962	Α
75	20191021tg01c_1962B.raw	10/23/2019 9:31	344.4	5.90	0.216	26.86744	25.92668	-25.05	25.39		2 A	1962	В
76	20191021tg01c_1962C.raw	10/23/2019 9:45	344.2	5.87	0.213	26.82842	26.12003	-25.09	25.57		2 B	1962	С
77	20191021tg01c_1962D.raw	10/23/2019 10:00	344.5	6.25	0.216	26.83362	25.91804	-25.09	25.36		2 B	1962	D
78	20191021tg01c_1962E.raw	10/23/2019 10:14	345	5.70	0.197	26.72792	25.52659	-25.20	24.95		2 B C	1962	E
79	20191021tg01c_1962F.raw	10/23/2019 10:29	344.9	5.95	0.209	26.60595	25.68311	-25.33	25.10		2 D	1962	F
80	20191021tg01c_1962G.raw	10/23/2019 10:43	344.6	5.66	0.192	26.80769	26.43055	-25.14	25.83		2 E	1962	G
81	20191021tg01c_1962H.raw	10/23/2019 10:58	344.5	5.56	0.194	26.76981	25.8011	-25.18	25.19		2 E F	1962	Н
82	20191021tg01c_1963A.raw	10/23/2019 11:12	344.6	5.58	0.194	27.07646	26.95645	-24.89	26.33		2 A B	1963	Α
83	20191021tg01c_1963B.raw	10/23/2019 11:27	344.8	5.60	0.195	27.04967	26.30661	-24.92	25.67		2 C	1963	В
84	20191021tg01c_1964A.raw	10/23/2019 11:41	344.1	5.35	0.184	26.98281	27.15967	-25.00	26.51		2 A	1964	Α
85	20191021tg01c_1964B.raw	10/23/2019 11:56	344.5	5.58	0.186	26.95439	26.56452	-25.03	25.90		2 B	1964	В
86	20191021tg01c_1964C.raw	10/23/2019 12:10	344.8	5.64	0.198	26.98491	26.62713	-25.01	25.94		2 B C	1964	С
87	20191021tg01c_1964D.raw	10/23/2019 12:25	344.5	5.81	0.201	27.06688	27.23853	-24.94	26.54		2 C D	1964	D
88	20191021tg01c_1964E.raw	10/23/2019 12:39	344.3	5.79	0.195	26.94214	26.54977	-25.07	25.83		2 D	1964	E

90 20101021 +c01c 106FA cour	10/22/2010 12:54	244.1	г ос	0.2	26 72706	27 61202	25.20	26.00	2 4	1965 A
89 20191021_tg01c_1965A.raw	10/23/2019 12:54	344.1	5.86		26.72786		-25.29	26.89	2 A	
90 20191021_tg01c_1965B.raw	10/23/2019 13:08	344.7	5.82	0.199		26.66887	-25.42	25.92	2 A	1965 B
91 20191021_tg01c_1965C.raw	10/23/2019 13:23	344.2	5.48		26.70379		-25.33	26.41	2 A 3 B	1965 C
10 20191120_tg01c_1965A.raw	11/20/2019 20:49	346.4	6.63	0.21	26.65	26.34	-24.83	26.30		1965 A
11 20191120_tg01c_1965B.raw	11/20/2019 21:03	346.6	5.88	0.20	26.47	26.52	-25.01	26.48	3 B	1965 B
12 20191120tg01c_1965C.raw	11/20/2019 21:18	346.6	5.89	0.20	26.45	25.97	-25.05	25.87	3 C	1965 C
13 20191120tg01c_1965D.raw	11/20/2019 21:32	346.9	6.25	0.21	26.56	26.32	-24.95	26.22	3 C	1965 D
14 20191120tg01c_1965E.raw	11/20/2019 21:46	346.8	5.51	0.19	26.53	26.59	-24.99	26.49	3 D	1965 E
15 20191120tg01c_1965F.raw	11/20/2019 22:00	346.8	6.07	0.20	26.55	26.62	-24.99	26.49	3 D	1965 F
16 20191120tg01c_1965G.raw	11/20/2019 22:14	346.7	6.48	0.21	26.57	26.81	-24.97	26.67	3 D	1965 G
17 20191120tg01c_1966A.raw	11/20/2019 23:21	347	6.33	0.21	26.12	26.38	-25.43	26.20	3 A	1966 A
18 20191120tg01c_1966B.raw	11/20/2019 23:35	346.5	5.75	0.19	26.24	27.05	-25.32	26.88	3 A B	1966 B
19 20191120tg01c_1967A.raw	11/20/2019 23:51	346.6	6.21	0.21	26.58	26.89	-24.99	26.70	3 A	1967 A
20 20191120tg01c_1967B.raw	11/21/2019 0:05	346.4	5.43	0.19	26.63	26.71	-24.96	26.48	3 A B	1967 B
21 20191120tg01c_1967C.raw	11/21/2019 0:20	346.7	5.94	0.20	26.64	26.63	-24.96	26.37	3 B	1967 C
22 20191120tg01c_1967D.raw	11/21/2019 1:00	346.7	6.42	0.21	26.52	25.94	-25.09	25.62	3 C	1967 D
23 20191120tg01c_1968A.raw	11/21/2019 1:14	347.2	6.11	0.21	26.27	26.11	-25.35	25.78	3 A B	1968 A
24 20191120tg01c_1968B.raw	11/21/2019 1:29	346.6	6.10	0.21	26.44	26.25	-25.20	25.90	3 C	1968 B
25 20191120tg01c_1968C.raw	11/21/2019 1:46	346.6	5.95	0.20	26.43	26.43	-25.21	26.07	3 D	1968 C
26 20191120tg01c_1969A.raw	11/21/2019 2:00	346.4	5.61	0.19	26.01	26.41	-25.64	26.03	3 A	1969 A
27 20191120tg01c_1969B.raw	11/21/2019 2:18	347	6.06	0.19	25.87	26.34	-25.79	25.93	3 B C	1969 B
28 20191120tg01c_1969C.raw	11/21/2019 2:36	346.5	6.00	0.20	25.20	25.87	-26.48	25.41	3 D E	1969 C
29 20191120tg01c_1970A.raw	11/21/2019 2:50	347	5.63	0.19	25.01	25.97	-26.68	25.50	3 A B	1970 A
30 20191120tg01c_1970B.raw	11/21/2019 3:04	346.7	6.03	0.19	25.08	25.93	-26.62	25.44	3 B C	1970 B
31 20191120tg01c_1971A.raw	11/21/2019 3:49	346.6	6.51	0.21	25.39	25.38	-26.32	24.83	3 A B C	1971 A
32 20191120tg01c_1972A.raw	11/21/2019 4:04	346.5	6.17	0.20	25.57	26.37	-26.14	25.86	3 A B	1972 A
33 20191120tg01c_1973A.raw	11/21/2019 4:18	346.4	5.39	0.19	25.36	25.54	-26.37	24.96	3 A B	1973 A
40 20191120tg01c_1973B.raw	11/21/2019 6:00	346.4	6.05	0.19	25.64	26.28	-26.16	25.59	3 B C	1973 B
41 20191120tg01c_1974A.raw	11/21/2019 6:32	346.4	6.43	0.21	25.78	25.83	-26.02	25.09	3 A B	1974 A
42 20191120tg01c_1974B.raw	11/21/2019 6:47	346.4	5.51	0.19	24.96	25.13	-26.86	24.34	3 C D	1974 B
43 20191120 tg01c 1975A.raw	11/21/2019 7:01	347.3	5.38	0.19	24.48	24.76	-27.35	23.92	3 A B	1975 A
44 20191120_tg01c_1975B.raw	11/21/2019 7:16	346.8	6.13	0.22	24.89	25.31	-26.95	24.48	3 C	1975 B
45 20191120_tg01c_1976A.raw	11/21/2019 7:30	346.7	5.79	0.19	24.88	25.50	-26.97	24.66	3 A	1976 A
46 20191120 tg01c 1976B.raw	11/21/2019 7:44	346.7	5.73	0.20	24.82	25.52	-27.04	24.67	3 B	1976 B
47 20191120 tg01c 1976C.raw	11/21/2019 7:58	346.7	6.71	0.21	24.84	26.26	-27.03	25.42	3 B C	1976 C
48 20191120_tg01c_1977A.raw	11/21/2019 8:13	346.7	5.41	0.19	25.11	28.77	-26.77	28.07	3 A	1977 A
49 20191120_tg01c_1977B.raw	11/21/2019 8:27	346.4	5.08	0.18	24.87	26.17	-27.02	25.29	3 A B	1977 B
50 20191120 tg01c 1978A.raw	11/21/2019 8:41	346.6	6.04	0.20	25.10	26.52	-26.80	25.64	3 A B	1978 A
51 20191120 tg01c 1978B.raw	11/21/2019 8:56	347.5	5.90	0.20	24.97	26.35	-26.93	25.45	3 A B D	1978 B
52 20191120 tg01c 1979A.raw	11/21/2019 9:10	346.4	6.25	0.21	25.44	25.50	-26.47	24.52	3 A B	1979 A
53 20191120 tg01c 1980A.raw	11/21/2019 9:24	346.9	5.39	0.20	25.30	26.92	-26.63	26.01	3 A B	1980 A
54 20191120 tg01c 1980B.raw	11/21/2019 9:38	346.7	6.23	0.21	25.48	26.88	-26.45	25.95	3 A B	1980 B
	,,, 5.50	,	0.25	01		_0.00	_31.10	_5.55		=====

55 20191120tg01c_1981A.raw	11/21/2019 9:53	346.8	5.63	0.19	25.21	26.05	-26.73	25.05	3 A B	1981 A
56 20191120tg01c_1981B.raw	11/21/2019 10:07	348.3	5.69	0.19	25.05	26.10	-26.90	25.08	3 B	1981 B
57 20191120tg01c_1981C.raw	11/21/2019 10:22	346.8	5.98	0.19	25.35	27.10	-26.61	26.12	3 A B C	1981 C
58 20191120tg01c_1982A.raw	11/21/2019 10:36	347.2	5.84	0.19	25.50	26.62	-26.46	25.60	3 A B	1982 A
59 20191120tg01c_1983A.raw	11/21/2019 10:50	347.5	5.84	0.20	25.52	26.07	-26.45	24.99	3 A B	1983 A
60 20191120tg01c_1983B.raw	11/21/2019 11:05	347.1	6.26	0.21	25.32	24.86	-26.66	23.70	3 C	1983 B
61 20191120tg01c_1983C.raw	11/21/2019 11:19	347.2	5.95	0.21	25.40	25.03	-26.58	23.86	3 C	1983 C
62 20191120tg01c_1983D.raw	11/21/2019 11:33	346.9	5.82	0.20	24.96	25.75	-27.03	24.61	3 D	1983 D
63 20191120tg01c_1984A.raw	11/21/2019 11:48	347.2	5.91	0.21	24.76	25.84	-27.24	24.68	3 A B C	1984 A
70 20191120tg01c_1985A.raw	11/21/2019 13:28	347	5.89	0.20	25.11	26.17	-26.93	24.94	3 A B	1985 A
71 20191120tg01c_1985B.raw	11/21/2019 13:43	347.5	6.09	0.21	24.93	25.84	-27.12	24.57	3 B	1985 B
72 20191120tg01c_1986A.raw	11/21/2019 13:57	347.2	5.03	0.18	25.06	26.58	-26.99	25.35	3 A B	1986 A
73 20191120tg01c_1987A.raw	11/21/2019 14:12	347.1	6.24	0.21	25.02	26.30	-27.04	25.03	3 A	1987 A
74 20191120tg01c_1987B.raw	11/21/2019 14:26	346.9	6.14	0.21	25.06	26.76	-27.01	25.51	3 B	1987 B
75 20191120tg01c_1987C.raw	11/21/2019 14:40	346.7	5.49	0.19	24.99	26.62	-27.08	25.35	3 B	1987 C
76 20191120tg01c_1988A.raw	11/21/2019 14:55	347.4	5.37	0.19	24.96	26.05	-27.12	24.73	3 A	1988 A
77 20191120tg01c_1988B.raw	11/21/2019 15:09	347	5.38	0.19	24.86	26.19	-27.22	24.87	3 A	1988 B
78 20191120tg01c_1989A.raw	11/21/2019 15:24	347.1	5.45	0.19	24.92	26.46	-27.16	25.15	3 A B	1989 A
79 20191120tg01c_1989B.raw	11/21/2019 15:38	346.7	5.33	0.19	25.28	26.80	-26.81	25.50	3 B	1989 B
80 20191120tg01c_1989C.raw	11/21/2019 15:53	346.6	5.76	0.20	25.11	26.64	-26.98	25.32	3 B	1989 C
81 20191120tg01c_1989D.raw	11/21/2019 16:07	347	5.61	0.20	24.90	26.99	-27.19	25.68	3 C	1989 D
82 20191120tg01c_1989E.raw	11/21/2019 16:22	346.5	5.13	0.18	25.08	27.52	-27.02	26.23	3 C	1989 E
83 20191120_tg01c_1989F.raw	11/21/2019 16:36	347.1	5.55	0.18	24.95	26.94	-27.15	25.60	3 C	1989 F
84 20191120_tg01c_1990A.raw	11/21/2019 16:51	347.2	5.34	0.19	24.88	27.23	-27.22	25.91	3 A	1990 A
85 20191120tg01c_1990B.raw	11/21/2019 17:05	347.6	5.31	0.18	24.97	26.71	-27.15	25.35	3 B	1990 B
86 20191120_tg01c_1990C.raw	11/21/2019 17:20	347.7	5.19	0.18	24.98	27.11	-27.14	25.77	3 B	1990 C
87 20191120_tg01c_1990D.raw	11/21/2019 17:34	347.3	5.82	0.20	25.24	27.14	-26.88	25.79	3 C	1990 D
88 20191120tg01c_1991A.raw	11/21/2019 17:49	347.6	5.72	0.20	25.10	26.88	-27.02	25.51	3 A	1991 A
89 20191120_tg01c_1991B.raw	11/21/2019 18:03	347.4	5.05	0.18	25.02	26.81	-27.11	25.42	3 A	1991 B
90 20191120_tg01c_1992A.raw	11/21/2019 18:18	347.3	5.80	0.20	25.54	27.40	-26.58	26.04	3 A B	1992 A
91 20191120tg01c_1992B.raw	11/21/2019 18:32	347.7	5.44	0.18	25.42	27.47	-26.71	26.11	3 B	1992 B
92 20191120tg01c_1992C.raw	11/21/2019 18:47	347.3	5.59	0.19	25.62	28.19	-26.51	26.86	3 C	1992 C
93 20191120tg01c_1992D.raw	11/21/2019 19:01	347.9	6.37	0.22	25.60	27.92	-26.53	26.57	3 C	1992 D
10 20191122tg01c_1993A.raw	11/22/2019 10:58	347.5	7.3777535	0.208	26.10354	27.22886	-26.2395	26.11565	4 A B C	1993 A
11 20191122tg01c_1994A.raw	11/22/2019 11:12	347.6	6.405857	0.205	25.90629	26.63779	-26.3256	25.48496	4 A B	1994 A
12 20191122_tg01c_1994B.raw	11/22/2019 11:26	347.8	5.898646	0.196	25.67138	26.02584	-26.493	24.8324	4 C	1994 B
13 20191122tg01c_1995A.raw	11/22/2019 11:41	347.5	6.294758	0.211	25.79904	26.75989	-26.4196	25.59156	4 A	1995 A

Appendix IV: Table of TG01C Isotope Data, 1775-1825:

position sample_ID		date_time	RT	amplitude	mass	c13	o18	c13c	o18c	run	subsamples included	year	assigned lette
14 20191122tg01c_17	75A.raw	11/22/2019 11:55	347.2	6.3172465	0.21	26.78935	27.82123	-25.46	26.69401		4 A	1775	Α
15 20191122tg01c_17	75B.raw	11/22/2019 12:09	347.7	6.079705	0.2	26.60598	27.71368	-25.6109	26.57057		4 B	1775	В
16 20191122tg01c_17	75C.raw	11/22/2019 12:23	347.9	4.6555225	0.201	26.74173	27.55748	-25.2774	26.39617		4 C	1775	С
17 20191122tg01c_17	75D.raw	11/22/2019 12:37	347.3	5.9504585	0.197	26.6125	27.85017	-25.5913	26.69263		4 D	1775	D
18 20191122tg01c_17	76A.raw	11/22/2019 12:51	347.2	5.849988	0.197	26.81956	27.69569	-25.3784	26.52017		4 A B	1776	Α
19 20191122tg01c_17	76B.raw	11/22/2019 13:06	347.1	6.561489	0.218	26.61336	27.5335	-25.6679	26.33969		4 B C	1776	В
20 20191122tg01c_17	76C.raw	11/22/2019 13:20	347.2	5.775767	0.193	26.80613	27.22071	-25.3849	26.00133		4 B C D	1776	С
21 20191122tg01c_17	77A.raw	11/22/2019 13:34	347.6	5.7646515	0.198	27.41906	27.62753	-24.7886	26.41781		4 A	1777	A
22 20191122tg01c_17	77B.raw	11/22/2019 13:48	347.4	5.889908	0.2	27.44397	27.55985	-24.7823	26.33671		4 B	1777	В
23 20191122tg01c_17	77C.raw	11/22/2019 14:02	347.5	6.177789	0.205	27.73904	27.34342	-24.5331	26.09972		4 C	1777	С
24 20191122tg01c_17	77D.raw	11/22/2019 14:16	347.6	5.8315535	0.202	27.63479	27.41006	-24.5925	26.15971		4 D	1777	D
25 20191122tg01c_17	77E.raw	11/22/2019 14:30	347.5	6.302538	0.202	27.51661	27.33221	-24.7683	26.06828		4 E	1777	E
26 20191122tg01c_17	77F.raw	11/22/2019 14:45	347.6	6.499327	0.218	27.22163	27.52014	-25.0805	26.25573		4 F	1777	F
27 20191122tg01c_17	77G.raw	11/22/2019 14:59	347.4	6.23229	0.205	26.76971	27.63578	-25.4903	26.36749		4 G	1777	G
28 20191122tg01c_17	77H.raw	11/22/2019 15:13	347.6	5.881131	0.201	26.6495	27.395	-25.5651	26.10557		4 H	1777	Н
29 20191122tg01c_17	78A.raw	11/22/2019 15:27	347.8	5.8574595	0.195	26.8519	27.94077	-25.3669	26.66873		4 A	1778	A
30 20191122tg01c_17	78B.raw	11/22/2019 15:41	347.8	5.5524865	0.188	27.3149	28.02602	-24.8776	26.74906		4 B	1778	В
31 20191122tg01c_17	78C.raw	11/22/2019 15:56	348.3	5.608374	0.189	27.51659	27.50909	-24.6909	26.19797		4 C	1778	С
32 20191122tg01c_17	79A.raw	11/22/2019 16:10	348.1	5.731497	0.203	26.56968	27.34116	-25.631	26.01308		4 A	1779	Α
33 20191122tg01c_17	79B.raw	11/22/2019 16:24	347.9	5.7891055	0.186	27.06641	27.43633	-25.1572	26.10431		4 B	1779	В
40 20191122tg01c_17	79C.raw	11/22/2019 18:03	347.7	5.4877645	0.197	27.36235	27.58884	-24.8443	26.20955		4 C	1779	С
41 20191122tg01c_17	79D.raw	11/22/2019 18:18	347.7	6.528568	0.219	27.18722	26.86147	-25.1492	25.43964		4 D	1779	D
42 20191122tg01c_17	80A.raw	11/22/2019 18:32	347.6	6.00374	0.201	26.15963	27.0176	-26.088	25.5965		4 A	1780	A
43 20191122_tg01c_17	80B.raw	11/22/2019 18:46	347.4	6.178366	0.202	26.24186	26.82987	-26.0323	25.39289		4 B	1780	В
44 20191122_tg01c_17	80C.raw	11/22/2019 19:00	347.1	6.0612925	0.211	27.1809	27.97474	-25.1063	26.58703		4 C	1780	С
45 20191122tg01c_17	80D.raw	11/22/2019 19:15	347	5.954756	0.21	26.75257	28.70662	-25.5122	27.34813		4 D	1780	D
46 20191122tg01c_17	81A.raw	11/22/2019 19:29	347.3	5.7937495	0.194	25.78562	30.95581	-26.435	29.70068		4 A	1781	A
47 20191122tg01c_17	81B.raw	11/22/2019 19:43	347.2	6.470318	0.219	27.22249	28.25373	-25.1231	26.86042		4 B	1781	В
48 20191122_tg01c_17	81C.raw	11/22/2019 19:57	346.9	5.7424615	0.194	26.4303	25.6941	-25.806	24.16963		4 C	1781	С
49 20191122tg01c_17	81D.raw	11/22/2019 20:12	346.9	6.2027385	0.202	27.16465	25.83486	-25.1525	24.31105		4 D	1781	D
50 20191122tg01c_17	81E.raw	11/22/2019 20:26	346.8	6.1314535	0.213	27.00777	26.70947	-25.299	25.22216		4 E	1781	E
51 20191122tg01c_17	81F.raw	11/22/2019 20:40	349	6.407557	0.218	26.04153	25.65078	-26.2755	24.10565		4 F	1781	F
52 20191122_tg01c_17	82A.raw	11/22/2019 20:54	347.7	5.21429	0.181	26.13519	27.21845	-26.0303	25.74366		4 A	1782	A
53 20191122tg01c_17	82B.raw	11/22/2019 21:09	347.2	6.441162	0.22	26.69222	26.80129	-25.6514	25.29995		4 B	1782	В
54 20191122_tg01c_17	82C.raw	11/22/2019 21:23	347.1	5.5196965	0.185	26.29042	26.61354	-25.9277	25.09682		4 C	1782	С
55 20191122_tg01c_17	83A.raw	11/22/2019 21:37	346.9	5.4724335	0.199	25.23475	26.58868	-26.9512	25.06448		4 A	1783	A
56 20191122_tg01c_17	83B.raw	11/22/2019 21:52	347.1	5.5316215	0.197	27.0111	27.14718	-25.2332	25.64389		4 B	1783	В
57 20191122_tg01c_17	83C.raw	11/22/2019 22:06	347.7	5.875031	0.188	27.08631	26.84324	-25.2083	25.31869		4 C	1783	С
58 20191122 tg01c 17	83D.raw	11/22/2019 22:20	347.8	6.2111815	0.207	26.60378	27.53027	-25.7228	26.03273		4 D	1783	D
59 20191122 tg01c 17		11/22/2019 22:35			0.217		27.65951		26.16163		4 A	1784	

60 20191122tg01c_1784B.raw	11/22/2019 22:49	347.6	5.518376	0.188	26.99714	27.52372	-25.2552	26.01244	4 B	1784 B
61 20191122tg01c_1784C.raw	11/22/2019 23:03	347.7	5.8684635	0.188	27.44829	27.41246	-24.8654	25.88882	4 C	1784 C
62 20191122 tg01c 1784D.raw	11/22/2019 23:18	347.7	6.271516	0.212	27.44005	27.8531	-24.9264	26.34387	4 D	1784 D
63 20191122 tg01c 1784E.raw	11/22/2019 23:32	347.4	6.903773	0.219	27.34788	27.66328	-25.0915	26.13751	4 E	1784 E
70 20191122 tg01c 1784F.raw	11/23/2019 1:13	347.6	5.7015845	0.196	27.1306	27.67017	-25.1739	26.08731	4 F	1784 F
71 20191122tg01c_1784G.raw	11/23/2019 1:27	347.6	6.1905505	0.204	26.77098	27.84637	-25.5886	26.26286	4 G	1784 G
72 20191122 tg01c 1785A.raw	11/23/2019 1:42	348	5.544262	0.187	26.73466	27.74621	-25.5423	26.14831	4 A	1785 A
73 20191122 tg01c 1785B.raw	11/23/2019 1:56	347.6	5.857618	0.2	27.26404	27.5361	-25.071	25.91818	4 B	1785 B
74 20191122 tg01c 1785C.raw	11/23/2019 2:10	347.8	6.024073	0.201	27.3925	27.55338	-24.9694	25.92633	4 C	1785 C
75 20191122 tg01c 1786A.raw	11/23/2019 2:25	347.7	5.906806	0.202	27.11232	28.12482	-25.2293	26.51545	4 A	1786 A
76 20191122 tg01c 1786B.raw	11/23/2019 2:39	347.7	5.4684875	0.188	27.13138	28.04765	-25.1542	26.42408	4 B	1786 B
77 20191122 tg01c 1786C.raw	11/23/2019 2:54	347.7	6.239367	0.208	27.16217	27.47559	-25.2265	25.81347	4 C	1786 C
78 20191122 tg01c 1786D.raw	11/23/2019 3:08	347.8	5.68059	0.191			-25.4173	25.24461	4 D	1786 D
79 20191122 tg01c 1786E.raw	11/23/2019 3:23	348.4	6.531865	0.218	26.51825			24.24538	4 E	1786 E
80 20191122 tg01c 1786F.raw	11/23/2019 3:37	347	6.5388595		27.04191	26.9845	-25.3851	25.26538	4 F	1786 F
81 20191122 tg01c 1786G.raw	11/23/2019 3:52	347.4	6.133906	0.207		26.2685		24.50307	4 G	1786 G
82 20191122 tg01c 1787A.raw	11/23/2019 4:06	347.2	6.3192725	0.212		28.49869		26.83057	4 A	1787 A
83 20191122 tg01c 1787B.raw	11/23/2019 4:21	347.2	6.2285835	0.215	26.9167	27.83633	-25.4759	26.12422	4 B	1787 B
84 20191122 tg01c 1787C.raw	11/23/2019 4:35	347.1	5.4325285	0.196	27.01663	28.10199	-25.2766	26.39102	4 C	1787 C
85 20191122 tg01c 1788A.raw	11/23/2019 4:50	347.1	6.315094	0.219		28.13597		26.41471	4 A	1788 A
86 20191122 tg01c 1788B.raw	11/23/2019 5:04	347	6.2728655			27.94476	-25.2138	26.2021	4 B	1788 B
87 20191122 tg01c 1789A.raw	11/23/2019 5:19	347.1	6.0488145		27.11724			25.86154	4 A	1789 A
88 20191122 tg01c 1789B.raw	11/23/2019 5:33	346.9	5.4223775	0.184	26.89338	26.9032	-25.4026	25.08523	4 B	1789 B
89 20191122 tg01c 1790A.raw	11/23/2019 5:48	346.9	6.1281765	0.208	26.58685	27.31115	-25.7958	25.50071	4 A B	1790 A
90 20191122 tg01c 1791A.raw	11/23/2019 6:02	346.9	5.30038	0.185		27.36194	-25.7661	25.5415	4 A	1791 A
91 20191122 tg01c 1791B.raw	11/23/2019 6:17	346.9	5.82874	0.21	26.78946			25.86513	4 B	1791 B
92 20191122 tg01c 1792A.raw	11/23/2019 6:31	346.8	5.7216365	0.203	26.54608	27.85133	-25.7888	26.02962	4 A	1792 A
93 20191122 tg01c 1792B.raw	11/23/2019 6:46	346.8	6.063174	0.196	26.58874	27.32471	-25.7932	25.46463	4 B	1792 B
10 20191123 tg01c 1793A.raw	11/23/2019 16:30	347.2	5.43		27.36954		-25.20	25.53	5 A	1793 A
11 20191123 tg01c 1793B.raw	11/23/2019 16:44	346.9	5.26	0.181	27.86195	29.11657	-24.73	26.87	5 B	1793 B
12 20191123tg01c_1794A.raw	11/23/2019 16:58	347.6	5.56	0.192	27.41875	29.06042	-25.15	26.80	5 A	1794 A
13 20191123 tg01c 1794B.raw	11/23/2019 17:12	347.6	5.40		27.43666		-25.14	24.71	5 B	1794 B
14 20191123 tg01c 1795A.raw	11/23/2019 17:27	347.6	5.09	0.186	26.75553	26.57196	-25.79	24.16	5 A	1795 A
15 20191123 tg01c 1795B.raw	11/23/2019 17:41	348.2	4.88	0.187	27.27801	26.86795	-25.29	24.45	5 B	1795 B
16 20191123 tg01c 1795C.raw	11/23/2019 17:55	347.3	5.92		27.22969		-25.34	25.21	5 C	1795 C
17 20191123 tg01c 1795D.raw	11/23/2019 18:09	347.3	5.69		27.51869		-25.07	24.77	5 D	1795 D
18 20191123tg01c_1795E.raw	11/23/2019 18:23	348.1	6.23	0.215	27.18353	27.60148	-25.39	25.18	5 E	1795 E
19 20191123 tg01c 1796A.raw	11/23/2019 18:37	346.8	5.70	0.194			-26.27	25.48	5 A	1796 A
20 20191123 tg01c 1796B.raw	11/23/2019 18:52	346.9	5.05		27.84205		-24.77	25.67	5 B	1796 B
21 20191123 tg01c 1796C.raw	11/23/2019 19:06	346.8	5.88	0.213	27.59061	27.37021	-25.01	24.89	5 C	1796 C
22 20191123 tg01c 1797A.raw	11/23/2019 19:20	346.8	6.33		26.76464		-25.80	24.78	5 A	1797 A
23 20191123 tg01c 1797B.raw	11/23/2019 19:34	346.8	5.57	0.194		27.21849	-25.83	24.70	5 B	1797 B
	,,5.0 .		2.07					= •		

24	20191123tg01c_1798A.raw	11/23/2019 19:48	347.2	6.29	0.218	26.57465	27.19976	-25.98	24.67	5 A	1798 A
25	20191123tg01c_1798B.raw	11/23/2019 20:02	346.9	5.47	0.186	27.31206	29.15624	-25.28	26.70	5 B	1798 B
26	20191123tg01c_1799A.raw	11/23/2019 20:17	347.1	5.79	0.203	26.58432	28.43748	-25.98	25.93	5 A	1799 A
27	20191123tg01c_1799B.raw	11/23/2019 20:31	347.2	5.91	0.204	26.9281	28.56229	-25.65	26.05	5 B	1799 B
28	20191123tg01c_1800A.raw	11/23/2019 20:45	346.8	5.97	0.206	26.71353	28.06826	-25.86	25.52	5 A	1800 A
29	20191123tg01c_1800B.raw	11/23/2019 20:59	347	6.20	0.217	27.39771	27.37087	-25.21	24.77	5 B	1800 B
30	20191123tg01c_1800C.raw	11/23/2019 21:13	347.1	6.11	0.209	27.81858	28.49029	-24.81	25.93	5 C	1800 C
31	20191123tg01c_1801A.raw	11/23/2019 21:28	347.3	6.14	0.21	27.39277	28.5985	-25.22	26.03	5 A	1801 A
32	20191123tg01c_1801B.raw	11/23/2019 21:42	347.3	5.71	0.2	27.766	27.9815	-24.87	25.37	5 B	1801 B
33	20191123tg01c_1801C.raw	11/23/2019 21:56	346.7	6.24	0.215	27.5714	27.24822	-25.05	24.59	5 C	1801 C
40	20191123tg01c_1802A.raw	11/23/2019 23:35	347.2	5.62	0.199	27.36052	27.9442	-25.27	25.23	5 A	1802 A
41	20191123tg01c_1802B.raw	11/23/2019 23:50	347.1	5.30	0.184	27.74218	28.77049	-24.91	26.09	5 B	1802 B
42	20191123tg01c_1803A.raw	11/24/2019 0:04	346.8	5.85	0.202	27.51645	28.80712	-25.13	26.11	5 A	1803 A
43	20191123tg01c_1803B.raw	11/24/2019 0:18	346.9	5.96	0.207	27.7325	28.87805	-24.93	26.18	5 B	1803 B
44	20191123tg01c_1804A.raw	11/24/2019 0:32	347	5.47	0.191	27.48455	28.5471	-25.17	25.82	5 A	1804 A
45	20191123tg01c_1804B.raw	11/24/2019 0:47	346.8	6.00	0.217	27.47208	28.57259	-25.18	25.84	5 B	1804 B
46	20191123tg01c_1804C.raw	11/24/2019 1:01	346.7	5.94	0.209	27.8434	28.64373	-24.83	25.90	5 C	1804 C
47	20191123tg01c_1805A.raw	11/24/2019 1:15	347.2	5.25	0.183	27.66335	28.95303	-25.01	26.21	5 A	1805 A
48	20191123tg01c_1805B.raw	11/24/2019 1:29	346.7	5.39	0.186	27.76172	28.30812	-24.92	25.53	5 B	1805 B
49	20191123tg01c_1805C.raw	11/24/2019 1:43	347.4	5.21	0.192	27.62224	28.92448	-25.05	26.16	5 C	1805 C
50	20191123tg01c_1806A.raw	11/24/2019 1:58	346.8	6.14	0.215	27.60775	28.95528	-25.07	26.19	5 A	1806 A
51	20191123tg01c_1806B.raw	11/24/2019 2:12	347	6.09	0.215	27.34435	28.77881	-25.33	25.99	5 B	1806 B
52	20191123tg01c_1807A.raw	11/24/2019 2:26	347	5.57	0.195	27.65387	29.20548	-25.03	26.43	5 A	1807 A
53	20191123tg01c_1807B.raw	11/24/2019 2:41	347.1	6.41	0.216	27.85341	29.21601	-24.85	26.43	5 B	1807 B
54	20191123tg01c_1808A.raw	11/24/2019 2:55	346.9	5.76	0.208	27.40719	28.57243	-25.28	25.75	5 A	1808 A
55	20191123tg01c_1809A.raw	11/24/2019 3:09	346.9	4.21	0.156	27.49575	28.90475	-25.20	26.09	5 A	1809 A
56	20191123tg01c_1810A.raw	11/24/2019 3:23	346.7	6.20	0.22	27.96097	28.56447	-24.76	25.73	5 A	1810 A
57	20191123tg01c_1810B.raw	11/24/2019 3:38	346.9	5.14	0.184	27.72629	28.4157	-24.98	25.56	5 A B	1810 B
58	20191123tg01c_1811A.raw	11/24/2019 3:52	347.2	5.10	0.184	27.15827	27.91106	-25.53	25.02	5 A	1811 A
59	20191123tg01c_1811B.raw	11/24/2019 4:06	347	5.46	0.19	26.98789	28.20609	-25.70	25.33	5 B	1811 B
60	20191123tg01c_1812A.raw	11/24/2019 4:21	346.7	5.59	0.196	27.25912	27.9858	-25.44	25.09	5 A	1812 A
61	20191123tg01c_1812B.raw	11/24/2019 4:35	347	5.98	0.212	26.82054	28.36806	-25.86	25.48	5 B	1812 B
62	20191123tg01c_1813A.raw	11/24/2019 4:49	347.1	5.43	0.188	26.98558	28.89463	-25.71	26.02	5 A	1813 A
63	20191123tg01c_1813B.raw	11/24/2019 5:04	347.2	6.16	0.214	27.20617	28.62997	-25.50	25.74	5 B	1813 B
70	20191123tg01c_1814A.raw	11/24/2019 6:45	347.2	5.65	0.199	27.43104	28.89925	-25.32	25.97	5 A	1814 A
71	20191123tg01c_1814B.raw	11/24/2019 6:59	347.5	6.08	0.21	27.44253	28.6667	-25.31	25.71	5 B	1814 B
72	20191123tg01c_1815A.raw	11/24/2019 7:14	347.4	5.98	0.211	27.46395	28.47139	-25.30	25.50	5 A	1815 A
73	20191123tg01c_1815B.raw	11/24/2019 7:28	347	5.79	0.206	27.89761	28.84857	-24.89	25.89	5 B	1815 B
93	20191123tg01c_1815C.raw	11/24/2019 12:18	347.4	5.34	0.185	27.78963	28.47316	-25.08	25.34	5 C	1815 C
74	20191123tg01c_1815D.raw	11/24/2019 7:43	347.1	6.22	0.217	27.85631	28.80423	-24.93	25.83	5 D	1815 D
75	20191123tg01c_1815E.raw	11/24/2019 7:57	346.8	5.71	0.204	27.59542	28.09697	-25.18	25.09	5 E	1815 E
76	20191123tg01c_1815F.raw	11/24/2019 8:12	347.4	6.07	0.207	26.97994	27.90461	-25.78	24.88	5 F	1815 F

77 20191123tg01c_1816A.raw	11/24/2019 8:26	347.3	5.68	0.2	27.42392	28.86175	-25.36	25.87	5 A	1816 A
78 20191123tg01c_1817A.raw	11/24/2019 8:40	346.9	6.19	0.219	27.24779	29.18216	-25.53	26.20	5 A	1817 A
79 20191123tg01c_1818A.raw	11/24/2019 8:55	347	5.72	0.203	27.59204	28.94528	-25.21	25.94	5 A	1818 A
80 20191123tg01c_1818B.raw	11/24/2019 9:09	347	5.49	0.194	27.43892	28.3972	-25.36	25.36	5 B	1818 B
81 20191123tg01c_1819A.raw	11/24/2019 9:24	347.3	5.76	0.203	27.28566	27.95555	-25.51	24.89	5 A	1819 A
82 20191123tg01c_1819B.raw	11/24/2019 9:38	347	5.48	0.193	27.39125	28.25573	-25.41	25.20	5 B	1819 B
83 20191123tg01c_1819C.raw	11/24/2019 9:53	346.8	6.21	0.216	27.44479	28.16973	-25.36	25.10	5 C	1819 C
84 20191123tg01c_1820A.raw	11/24/2019 10:07	347.4	5.93	0.214	26.70532	27.7904	-26.07	24.69	5 A	1820 A
85 20191123tg01c_1820B.raw	11/24/2019 10:22	347.4	5.17	0.183	27.19979	28.64998	-25.61	25.59	5 B	1820 B
86 20191123tg01c_1821A.raw	11/24/2019 10:37	347.3	5.66	0.205	27.43036	28.9366	-25.39	25.88	5 A	1821 A
87 20191123tg01c_1821B.raw	11/24/2019 10:51	347.6	5.42	0.194	26.91739	28.35343	-25.89	25.26	5 B	1821 B
88 20191123tg01c_1822A.raw	11/24/2019 11:06	348.1	5.38	0.19	27.10406	27.92435	-25.71	24.80	5 A	1822 A
89 20191123tg01c_1823A.raw	11/24/2019 11:20	347.6	5.28	0.186	26.59836	28.20844	-26.20	25.09	5 A	1823 A
90 20191123tg01c_1823B.raw	11/24/2019 11:35	347.5	5.87	0.208	26.93447	28.44691	-25.88	25.33	5 B	1823 B
91 20191123tg01c_1824A.raw	11/24/2019 11:49	347.5	6.00	0.216	27.51542	28.91582	-25.33	25.82	5 A B	1824 A
92 20191123tg01c_1825A.raw	11/24/2019 12:04	347.7	6.03	0.206	26.95556	28.30612	-25.87	25.17	5 A B	1825 A